2018-02-12

Serum proteases potentiate BMP-induced cell cycle re-entry of dedifferentiating muscle cells during newt limb regeneration

Wagner, Ines; Wang, Heng; Weissert, Philipp; Straube, Werner; Shevchenko, Anna; Gentzel, Marc; Brito, Gonçalo M; Tazaki, Akira; Oliveira, Catarina; Sugiura, Takuji; Shevchenko, Andrej; Simon, András; Drechsel, David; Tanaka, Elly

Dev Cell. 2017 Mar 27;40(6):608-617.e6.
http://doi.org/10.1016/j.devcel.2017.03.002
http://hdl.handle.net/10616/46223

Serum proteases potentiate BMP-induced cell cycle re-entry of dedifferentiating muscle cells during newt limb regeneration

Ines Wagner[1,2,6*], Heng Wang[3*], Philipp M. Weissert[1,2,5*], Werner L. Straube[1,*], , Anna Shevchenko[1], Marc Gentzel[1], Goncalo Brito[3], Akira Tazaki[2], Catarina Oliveira[1,2], Takuji Sugiura[2], Andrej Shevchenko[1], András Simon[3,4], David N. Drechsel[1,4], Elly M. Tanaka[2,4]

*These authors contributed equally to this work.

[1]Max Planck Institute of Molecular Cell Biology and Genetics, Dresden Germany

[2]Technische Universität Dresden, DFG Research Center for Regenerative Therapies, Dresden Germany

[3]Karolinska Institute, Department of Cell and Molecular Biology, Centre of Developmental Biology for Regenerative Medicine

Current Address:

[5]European Research Institute for the Biology of Ageing, University Medical Centre Groningen, University of Groningen, Groningen, the Netherlands

[6]DKMS Life Science Lab, Fiedlerstrasse 34, Dresden, Germany

[4]Authors for correspondence and current address:

Lead contact:
Elly M. Tanaka
Institute of Molecular Pathology (IMP)
Campus Vienna Biocenter 1
1030 Vienna, AUSTRIA
Tel: + +43 1 797303200
E-mail: elly.tanaka@imp.ac.at

David N. Drechsel
Institute of Molecular Pathology (IMP)
Campus Vienna Biocenter 1
1030 Vienna, AUSTRIA
Tel: + +43 1 797303200
E-mail: david.drechsel@imp.ac.at

András Simon
Karolinska Institute, Department of Cell and Molecular Biology, Centre of Developmental Biology for Regenerative Medicine,
Berzelius väg 35
17177 Stockholm, SWEDEN

Email: Andras.Simon@ki.se

Key words: Limb Regeneration, plasmin, thrombin, BMP (Bone Morphogenetic Protein), dedifferentiation, salamander, cell cycle re-entry

ABSTRACT

Limb amputation in the newt induces myofibers to dedifferentiate and re-enter the cell cycle to generate proliferative myogenic precursors in the regeneration blastema. Here we show that Bone Morphogenetic Proteins (BMP) and mature BMPs that have been further cleaved by serum proteases induce cell cycle entry by dedifferentiating newt muscle cells. Protease-activated BMP4/7 heterodimers that are present in serum strongly induced myotube cell cycle re-entry with protease cleavage yielding a thirty-fold potency increase of BMP4/7 compared to canonical BMP4/7. Inhibition of BMP signaling via muscle-specific dominant-negative receptor expression reduced cell cycle entry *in vitro*, and *in vivo*. *In vivo* inhibition of serine protease activity depressed cell cycle reentry, which in turn was rescued by cleaved-mimic BMP. This work identifies a mechanism of BMP activation that generates blastema cells from differentiated muscle.

INTRODUCTION

In several regeneration contexts, cells of mature phenotype re-enter the cell cycle to help regenerate missing structures. After lentectomy in the newt, dorsal iris pigmented epithelial cells (PEC) lose pigmentation, re-enter the cell cycle and transdifferentiate to regenerate the lens (Okada, 1991) (Grogg et al., 2005). During heart regeneration, cardiac myocytes re-enter the cell cycle and apparently expand to replace injured tissue (Jopling et al., 2010; Kikuchi et al., 2010). During newt limb regeneration, skeletal muscle fibers dedifferentiate by cellularization of syncytial muscle fibers, down-regulation of muscle-specific proteins, and re-entry into the cell cycle to generate proliferative blastema cells, a process involving cell death-related pathways (Sandoval-Guzman et al., 2014) (Wang et al., 2015). The molecular pathways that initiate proliferation of dedifferentiating skeletal muscle and how the signal is activated by limb amputation remains poorly characterized. Recent findings have identified a MARCKS (Myristoylated alanine-rich C-kinase substrate)-like protein as an epithelially-expressed factor that stimulates proliferation of both resident stem cells as well as of dedifferentiated myofibre progeny (Sugiura et al., 2016). Given that the repression of many of the canonical signalling pathways inhibits regeneration, the possibility that injury-activation of a canonical pathway was also involved lay open (Beck et al., 2001; Lin and Slack, 2008) (Poss, 2010).

The local activities of serum proteases that regulate blood clotting are associated with initiation of regeneration. Regenerating newt limbs show localization of thrombin proteolytic activity (Tanaka et al., 1999) and inhibition of thrombin

activity repressed iris PEC proliferation (Imokawa and Brockes, 2003) (Godwin et al., 2010). *In vitro*, newt skeletal myotubes re-entered cell cycle after exposure to serum, an effect that was strongly potentiated by thrombin and plasmin treatment (Tanaka et al., 1999; Tanaka et al., 1997). These results implied that circulating plasma contains a cell cycle inducing activity that is highly activated by proteolytic cleavage. Biochemical characterization and partial purification of the activity indicated that it is a high molecular weight glycoprotein with defined chromatographic properties (Straube et al, 2004).

An important goal motivated by these results has been to identify the substrates of clotting proteases that induce cell cycle re-entry during regeneration. Is there a growth stimulatory factor that is a direct protease target, or do serum proteases act indirectly by cleaving an inhibitor? Here by assaying newt skeletal myotube cell cycle re-entry we show that BMP4-containing heterodimers as the major serum component required and sufficient for myotube cell cycle re-entry. We further show that BMPs have at least two major cleavage sites that are differentially sensitive to thrombin and plasmin. The combined cleavage results in up to thirty-fold potency increase of BMP4/7. *In vivo* blockage of BMP signaling specifically in dedifferentiating muscle fibers negatively affects S-phase entry. Furthermore, the in vivo inhibition of serum protease activity depresses the BMP-dependent S-phase entry that is in turn rescued by a cleaved-mimic BMP. An additional, and in a broader context, significant conclusion of our quantitative studies is that the detection of serum BMP4 has previously been underestimated by up to 1000-fold due to unrecognized lack of the N-terminal epitopes of serum BMPs used for ELISA quantification.

RESULTS

Potent forms of BMP4-containing dimers in serum stimulate newt myotube S-phase re-entry

The application of fractionated serum samples to cultured newt myotubes results in their concentration-dependent re-entry into S-phase, quantitated as the percentage of myotubes incorporating BrdU during a 12 hours pulse (Tanaka et al., 1997). We used this quantitative myotube response to measure the amount of "S-phase Re-entry inducing Factor" (SPRF), in different fractions from serum. By quantitating activity versus total protein concentration we had previously found that SPRF activity is enriched by 20-fold over serum in commercially produced, low-purity bovine thrombin preparations and that it was possible to separate SPRF from its activator using several different chromatographic methods (Tanaka et al., 1999)(Straube et al, 2004). To molecularly identify SPRF, the thrombin preparation was subjected to four sequential steps of column chromatography (Figure S1A). The specific activity of SPRF was measured across sequential fractions from each column and fractions containing the peak of activity were pooled and applied to the next chromatography step. "Fold purification" was calculated based on the fold increase in specific activity found in the peak pool and "yield" was calculated based on the total amount of activity found in the peak pool from each step (Figure S1A). The most purified fraction was subjected to non-reducing SDS-PAGE. Mass spectrometry analysis of trypsin-digested proteins of the gel regions between 28-39 kD identified 34 major proteins that included BMP4, BMP5, and BMP7 (Table S3). A visual screen of 16 commercially available recombinant proteins on the myotube assay suggested

that only BMP4 could induce a myotube response. To determine if the presence of BMP4 correlated with the increased purification of SPRF, we performed western blotting after loading equal amounts of total protein from the peak pools on SDS PAGE. The starting material and peak pool from the cation exchange step showed undetectable levels of BMP4 whereas we observed a highly enriched representation of BMP4 in the last two column steps (Figure S1B). Western blotting across the last size exclusion fractionation (equal volume loading of samples) showed correlation between the BMP4 signal and the S-phase re-entry activity (Figure S1D). BMP5, BMP6 and BMP7 were not detectable using currently available ELISA and western blot reagents, BMP2 which is in the same subfamily as BMP4 and very similar in sequence was detected in the most purified fractions although it had not been detected by MS (Figure S1C). These results indicated that the presence of BMP4 and possibly BMP2 correlated quantitatively with the presence of SPRF activity during the purification.

To determine if BMP4 accounts for at least part of the SPRF activity, we assayed recombinant bovine BMP4 homodimers (bBMP4/4) on newt myotubes but surprisingly high concentrations were required to elicit a response. Recombinant bBMP4/4 and bBMP7/7, individually or in combination stimulated 50% maximal S-phase response at 47 to 77 ng/ml (1.9 to 3.0 nM) (Figure 1A). In contrast the native bBMP4 present in the SPRF purification fractions induced 50% maximal S-phase response at an apparent concentration of 0.06 ng/ml (2.4 pM) (Figure 1A). These results suggested that either native BMP4 containing dimers were intrinsically more potent than recombinantly produced proteins, or accessory factors work in parallel to or in concert with native BMPs to account for their

increased potency. To investigate this discrepancy we first assayed recombinant bBMP4/7 heterodimers. Consistent with previous reports (Israel et al., 1996) that BMP heterodimers have higher activity than homodimers, the recombinant bBMP4/7 heterodimer showed approximately 19-fold higher potency when compared with recombinant bBMP4/4 homodimer (Figure 1A, Figure S2A) but this still left a 40-fold discrepancy in activity between native BMPs in the purified SPRF material and the recombinant BMP preparations.

To determine if BMPs represent a major part of the activity in the serum preparations, we added recombinant noggin-FC, a stoichiometric, pan-specific inhibitor of BMPs (Holley et al., 1996; Zimmerman et al., 1996), to both partially purified SPRF and to recombinant bBMP preparations, and found extinction of activity (Figure 1B). Noggin-Fc also inhibited the cell cycle re-entry activity present in fetal calf serum (Figure S2B). Using noggin-FC as an affinity reagent, we specifically depleted BMPs from a partially purified SPRF preparation and found depletion of activity that could be quantitatively recovered using 1% SDS as eluate (Figure 1C). The eluate was separated on non-reducing SDS-PAGE, proteins were retrieved from gel slices and recovery of bioactivity found in the size range of 28-36 kD in this eluate (Figure 1D). Mass spectrometry analysis of this gel slice identified BMP2, BMP4, BMP5, BMP6 and BMP7.

We then specifically immunodepleted BMP4 from the Butyl20 fraction using polyclonal antibodies and correspondingly observed a loss of activity which could be quantitatively recovered from the immunoprecipitate (Figure 1E). This result shows that BMP4-containing homo- or heterodimers are a major and

sufficient constituent of the activity. Mass spectrometry analysis of the active region of a non-reducing gel between 28 and 36 kD identified BMP2, BMP4, BMP5, BMP6 and BMP7 (Table S1). Since no detectable cross-reaction of the anti-BMP4 antibody was observed with BMP5, BMP6 and BMP7 these results strongly suggest that the serum preparations contain BMP2/4, BMP4/5, BMP4/6 and BMP4/7 heterodimers. Taken together these results show that BMP-containing dimers account for the SPRF activity and are sufficient for cell cycle re-entry in newt myotubes.

Activated BMPs are cleaved at multiple target sites by thrombin and plasmin

Considering the large discrepancy in potency between serum-derived BMPs versus recombinant BMP4/7, and earlier observations that the serum factor is activated by thrombin and plasmin proteolysis, we investigated whether BMPs are direct targets of thrombin and plasmin. The treatment of recombinant hBMP4/7 with purified thrombin resulted in a 10-15-fold increase in activity while treatment with plasmin resulted in a 20-30-fold increase in activity (Figure 2A). Plasmin and thrombin also induced increased potencies in the recombinant hBMP2/2, hBMP4/4 and hBMP7/7 (Figure 2B, Figure S2C-D). We noticed in western blots reduced signal for protease treated BMP2, BMP4 and BMP7 (Figure 2C) which could have reflected either a general proteolytic degradation of proteins or an alteration of a major epitope for antibody binding. We therefore analyzed purified, bacterially-produced recombinant hBMP4/4 after plasmin or thrombin treatment by silver staining versus western blot. Human BMPs were the only available preparations with sufficient purity for such

detailed biochemical analysis and are practically identical in sequence to bovine BMP4 (1 amino acid substitution) so we performed the analyses in Figure 2 and subsequent work with human recombinant BMPs. Silver staining showed a progressive appearance of multiple lower molecular weight bands with increased incubation with plasmin and thrombin, but the overall protein level remained constant, excluding generalized proteolytic degradation, but rather suggesting that an alteration of the epitope responsible for antibody binding (Figure 2D).

We next pursued mapping the target sites on BMP4 for thrombin and plasmin. Thrombin cleaves the peptide bond following positively charged residues with high selectivity while plasmin cleaves the peptide bond following lysine or arginine residues with relatively relaxed surrounding sequence requirements (Mattler and Bang, 1977; Ryan et al., 1976; Vindigni, 1999). The BMP4 N-terminus contains multiple lysine and arginine residues, which when cleaved would cause the N-terminus to be cleaved into small fragments and released (Figure S3). This N-terminal domain has previously been characterized as a heparin-binding domain that causes BMP retention in heparin-containing gels and can be removed by plasmin treatment, which results in higher BMP2 bioactivity on alkaline phosphatase induction assay (Ruppert et al., 1996; Uludag et al., 2001) (Roedel et al., 2013). In addition BMP4 also contains lysine residues in the centrally (K78) and in the C-terminus (K99, K103) with the K103 site representing an ideal plasmin substrate sequence, conserved among BMPs . Due to intramolecular disulfide bonding, the peptides resulting from such cleavages

244 are predicted to remain covalently associated with the mature dimer (Figure
245 S3E).
246
247 To map the thrombin and plasmin–associated cleavage sites we employed
248 Edman sequencing of hBMP4/4 and hBMP4/7, which detects newly generated N-
249 terminal amino acids after protein cleavage. We first analyzed hBMP4/4 to
250 understand cleavage sites on the BMP4 polypeptide alone. The untreated sample
251 yielded the sole presence of the classical N-terminus of the mature BMP4, SPKHH
252 (Figure S3A, pink, Data S1, Table S2). Thrombin treated BMP4/4 revealed a
253 single new N-terminus -ARKKNK- as (Figure S3A, green, Data S1, Table S2)
254 indicating that thrombin targets arginine (R8) which is also consistent with gel
255 mobility data (Figure 2D, Figure S3B). In contrast, plasmin-treated BMP4/4
256 yielded two N-termini, KKNKN, and NYQEM indicating that plasmin targets R10
257 and K103 (Figure S3A, orange, Data S1, Table S2) consistent with gel mobility
258 data showing the appearance of two major lower molecular weight peptides
259 (Figure S3B). These findings suggest that the increased potency of plasmin-
260 treated BMPs derives from the additional cleavage at K103 (Figure S3A , Data S1,
261 Table S2).
262
263 To confirm the C-terminal plasmin site, we also performed mass spectrometry
264 and compared the presence of peptides in preparations that had or had not been
265 reduced and alkylated (to break disulfide bridges and prevent their re-
266 formation). The C-terminal peptides NYQEMVVEGCGCR and some traces of
267 VVLKNYQEMVVEGCGCR were the major peptides detected in the plasmin-
268 treated samples that had been reduced and alkylated but were not present in the

non-reduced samples. This result confirms the occurrence of plasmin-mediated cleavage at the C-terminal K99 and/or K103 residues and retention in the native dimer via disulfide bonds.

Since we had observed a high shift in potency of plasmin-cleaved BMP4/7 (Figure 2A, Figure S3C), we performed Edman sequencing of the plasmin derived non-reduced recombinant human BMP4/7 to determine cleavage sites in BMP7. The analysis yielded the BMP4 sequences -NYQEM- and -KKNKN as well as three BMP7 sequences, DLGWQDW, MANVAEN, NMVVRAC, indicating cleavage of BMP7 in several internal locations (Figure S3A, Data S1, Table S2). These results show that BMP4 and BMP7 have plasmin cleavage sites beyond the previously known N-terminal K8 sequence on BMP2 (Roedel et al., 2013; Uludag et al., 2001). Cleavage at these sites maintains an intact BMP molecule in the disulfide bonded state, and correlates with the increased ability of plasmin to activate the BMP4/7 heterodimer.

In vivo cell cycle entry of dedifferentiating muscle involves SMAD-mediated BMP signaling and is protease-sensitive

To test the role of BMP signaling in S-phase entry of skeletal muscle cells *in vivo*, we sought to autonomously block BMP signaling in newt skeletal muscle fibers by expression of dominant negative BMP receptors (dnBMPR). To validate the dnBMPRs, we first transfected myotubes *in vitro* with *dnAlkLK2, dnAlkLK3 and dnAlkLK6* expression constructs together with a *nucGfpFP* construct and then challenged them 24 hours after plating with recombinant hBMP4/7. In control samples transfected with *nucGfpFP* only, S-phase response in GFP⁺ myotubes

Formatted: Font: Italic

Formatted: Font: Italic

Formatted: Font: Italic

was 24±4%. In contrast all tested dnBMPR including *dnAlkLK2*, *dnAlk3* and *dnAlkLK6* yielded strong suppression of the S-phase response to 2.0 ± 1.8% ($p = 2.26 \times 10^{-08}$), 6.5 ± 4.6% ($p = 7.12 \times 10^{-09}$) and 0.2 ± 0.6% ($p = 7.47 \times 10^{-08}$) respectively (Figure 3A). These results indicate that blockage of BMP signaling within the myotube is sufficient to block the S-phase response.

To block signaling *in vivo*, we specifically expressed DNA constructs in newt skeletal muscle fibers via the co-electroporation of a muscle-specific *MCK:cre*, a loxP expression cassette *CAGGs: loxP-Cherry 3PA-loxP-Histone2B-YFP* or *CAGGs: loxP-Cherry 3PA-loxP-Histone2B-YFP-T2A-dnALK* flanked by Tol2 transposon sites, and a Tol2 transposase expression plasmid (Sandoval-Guzman et al., 2014). This procedure yields expression of the H2B-YFP and dnALKs specifically in MHC^{+} muscle fibers of the intact limb. Upon limb amputation, muscle fibers cellularize prior to S-phase entry yielding YFP^{+}/MHC^{-} proliferating cells in the regeneration blastema as assessed by PCNA staining and by incorporation of nucleotide analogues (Sandoval-Guzman et al., 2014). To assay DNA synthesis in cells deriving from labeled fibers, electroporated limbs were injected daily with EdU 8-13 days post-limb amputation prior to harvesting (Figure 3B). In control limbs expressing H2B-YFP alone, 67.2±6.8% of muscle derived $YFP^{+}MHC^{-}$ cells in the blastema had incorporated EdU (Figure 3C-E). In contrast, expression of dnALK2, dnALK3 or dnALK6 with H2B-YFP yielded a lower EdU labeling index of 47 ± 7.6% ($p = 0.1106$), 41 ± 8.4%($p = 0.0522$), 43.2 ± 6.2% ($p = 0.042$), respectively, indicating the participation of BMP signaling during S-phase of skeletal muscle derived cells (Figure 3E). These results indicated that BMP

Formatted: Font: Italic

Formatted: Font: Italic

318 signaling is acting to promote cell cycle re-entry *in vivo* in dedifferentiating
319 muscle cells.
320
321 To determine whether the BMP signaling proceeded via intracellular SMAD
322 activity we used a SMAD-luciferase reporter (Collery and Link, 2011;
323 Korchynskyi and ten Dijke, 2002). Cultured newt myotubes transfected with the
324 reporter displayed a BMP4/7-dependent induction of luciferase activity. This
325 response was blocked by provision of the BMP-inhibitor, noggin, indicating that
326 the newt myotube response to BMP activates SMAD signaling (Figure 4A).
327 Transfection of this reporter *in vivo* into the limb blastema also showed
328 increased reporter activity during the stage of muscle dedifferentiation, at 6 and
329 12 days post-amputation (Figure 4B). The limb blastema consists of cells
330 deriving from different tissues. To directly determine if SMAD signaling takes
331 place in dedifferentiating muscle cells, we labeled muscle fibers with H2B-YFP
332 via electroporation as described above and performed immunofluorescence
333 staining for nuclear pSMAD1/5/8 staining. As shown in Figure 4C, YFP^+ cells
334 showed nuclear pSMAD1/5/8 staining confirming the implementation of SMAD
335 activity during muscle dedifferentiation.
336
337 We next aimed to examine the relevance of BMP protease activation to *in vivo*
338 muscle cell cycle re-entry. We first assessed *in vitro* the relative effectiveness of
339 recombinantly produced WT BMP to a mutant BMP lacking the N-terminus (ΔN-
340 BMP4**)** that mimics the N-terminally cleaved form by assaying identically
341 produced proteins in the linear range on myotubes. Volume for volume the ΔN-
342 BMP4 more potently induced cell cycle re-entry than the full-length protein

(Figure 4D). Mutations in the C-terminal site prevented efficient production of secreted BMP and therefore, this C-terminal cleavage could not be analysed by mutational analysis (data not shown).

We then compared the *in vivo* effectiveness of the WT and ΔN forms to accelerate dedifferentating myofiber cell cycle entry by overexpressing the BMPs in the early blastema and then assaying the proliferation of muscle cell progeny by MCM2 staining at 13 dpa. Injection of equal amounts of baculovirus for the two constructs showed a higher proliferation index of dedifferentiating muscle-derived cells in samples expressing ΔN-BMP4 compared to the full length BMP4 (Figure 4F,G). Finally we asked if inhibition of serine proteases in the amputated limb reduced cell cycle entry of muscle-derived cells upstream of BMP. Injection of YFP-muscle-labeled limbs with AEBSF, an irreversible inhibitor of both thrombin and plasmin (Powers et al., 2002), depressed EdU incorporation in YFP^+ muscle fiber-derived cells compared to PBS-injected limbs (Figure S4A,B). Expression of the ΔN-BMP4 restored EdU incorporation in YFP^+ muscle fiber-derived cells showing that serine protease activity acts upstream of cleaved-BMP-dependent muscle cell cycle re-entry (Figure S4C). This epistasis analysis confirms a role for protease activity as a positive, upstream regulator of BMP-driven induction of the cell cycle during limb regeneration.

DISCUSSION

Here we identify BMPs as serum factors that can stimulate cell cycle entry of differentiated newt skeletal myotubes and muscle fibers, a key step in muscle dedifferentiation during limb regeneration. We further show that BMP activity is

potentiated by cleavage mediated by thrombin and plasmin. These observations lead to a model in which resting skeletal muscle fibers in the intact limb remain sequestered from plasma BMPs that are circulating within intact blood vessels. Limb amputation damages the endothelium that leaks plasma BMPs into surrounding tissues and initiates the clotting cascade triggering not only fibrin clot formation, but also proteolytic processing of BMPs. The progeny of the damaged muscle fibers are exposed to and respond to these activated BMPs with cell cycle re-entry.

The expression of BMP4 is also upregulated early after limb amputation in Xenopus and Axolotl which would also be a target of activating proteolysis, further reinforcing BMP action during early regeneration (Beck et al., 2006; Guimond et al., 2010; Knapp et al., 2013) (Kochegarov et al., 2015). Another potential BMP source is peripheral nerves, as BMP2 and BMP7 were shown to substitute a proregenerative role of nerves in the accessory limb model and are expressed in DRG neurons (Makanae et al., 2014). Two inhibition studies implicated BMP signaling in early steps of limb regeneration, but since inhibition of the pathway had been elicited by global expression of noggin, it was unclear if the negative effects on cell proliferation had been through a direct or indirect means (Beck et al., 2006; Guimond et al., 2010; Knapp et al., 2013). Here. through cell autonomous inhibition of BMP signaling, we show a direct effect of the pathway on muscle-derived cell cycle entry. This pathway appears to be working in parallel to the recently described MLP pathway (Sugiura et al., 2016) which would explain the partial loss of EdU incorporation when we blocked BMP signaling in in vivo muscle fibers, while we observed complete block of S-phase

393 in response to serum in the in vitro assay system, where MLP was not present in
394 the culture.
395
396 In other biological systems, recombinant BMP4/4 had been used to implicate
397 BMP4/4 as a potential bioactive serum factor that could support mouse ES cell
398 pluripotency and the conversion of oligodendrocyte precursors into a neural
399 stem-like cell, but a paradox existed in which the concentrations of recombinant
400 BMPs required for cell stimulation did not match the very low concentrations of
401 BMPs measured in serum (Kondo and Raff, 2000; Ying et al., 2003) (Park et al.,
402 2008; Tacke et al., 2007; Wendling et al., 2007). Therefore it was unclear
403 whether other serum factors were really required. Our biochemical approach
404 provides an explanation that could resolve this controversy. First we show that
405 in our *in vitro* assay, serum BMPs quantitatively account for the activity. Our
406 work also strongly suggests that a significant fraction of the BMP4 in serum is
407 complexed to BMP5, 6 and 7 as heterodimers. This is important considering that
408 BMP4/7 is more potent than BMP4/4 in our and other cellular assays. Next our
409 work indicates that the quantification of serum BMPs by western blot or ELISA
410 vastly underestimates the concentration of BMPs in serum. ELISAs used to
411 quantitate BMP4 and BMP7 employ antibodies that are directed against the N-
412 terminus. Our work shows that since the N-terminus is lacking in serum BMPs,
413 the vast majority of BMPs present in serum are likely not detected. Using ELISA
414 kits, the serum concentration of BMP4 has been estimated at 0.04 ng/ml and
415 BMP7 at 0.01-0.28 ng/ml (Park et al., 2008; Tacke et al., 2007; Wendling et al.,
416 2007). Based on our measurements of the loss of immunoreactivity in western
417 blots using a commercial polyclonal anti-BMP antibody, and the enrichment of

BMP activity along the different steps of purification, we calculate that BMP4 is present in serum at a concentration of 20-100 ng/ml, which is 1000-fold higher than previous estimations. Significantly, the re-estimated concentration of this molecule is at levels highly relevant to cellular assays.

In summary, our work provides insight into how a local injury initiates activation of the BMP signaling pathway and how this signaling pathway acts directly on a cellular mechanism involved in generating blastema cells from mature tissue, namely cell cycle entry during dedifferentiation of muscle fibers. This molecular insight has important implications for promoting a proliferative state for the purpose of regeneration.

EXPERIMENTAL PROCEDURES

See STAR methods page.

ACKNOWLEDGEMENTS: This work was supported by BMBF Biofutures (EMT), MPI-CBG (EMT, DND, ASh) and the CRTD (EMT) and by the Swedish Research Council, Wenner-Gren Foundation and Cancerfonden to ASi. We thank Walter Sebald for bacterially expressed human BMP2/2 and BMP4/4, and Barbara Borgonova, Mike Tipsword, Regis Lemaitre and Elena Taverna for technical assistance and Michael Kiess (Toplab GmbH) for Edman sequencing.

AUTHOR CONTRIBUTIONS: IW, PW, WLS, AT, ~~MG, ASh,~~ TS, DND performed and analyzed in vitro BMP characterization and myotube assays. MG, Anna Shev., Andrej Shev. performed mass spectrometry analysis. HW, GC~~, CO~~ performed in

vivo newt experiments. CO made baculovirus for in vivo experiments IW, HW, ASimon, EMT analysed data and wrote the manuscript.

445 **References**

446 Beck, C.W., Christen, B., Barker, D., and Slack, J.M. (2006). Temporal requirement
447 for bone morphogenetic proteins in regeneration of the tail and limb of Xenopus
448 tadpoles. Mech Dev *123*, 674-688.
449 Beck, C.W., Whitman, M., and Slack, J.M. (2001). The role of BMP signaling in
450 outgrowth and patterning of the Xenopus tail bud. Dev Biol *238*, 303-314.
451 Collery, R.F., and Link, B.A. (2011). Dynamic smad-mediated BMP signaling
452 revealed through transgenic zebrafish. Dev Dyn *240*, 712-722.
453 Ferretti P, Brockes JP. (1988). Culture of newt cells from different tissues and
454 their expression of a regeneration-associated antigen. J Exp Zool. *247,* 77-91.
455 Godwin, J.W., Liem, K.F., Jr., and Brockes, J.P. (2010). Tissue factor expression in
456 newt iris coincides with thrombin activation and lens regeneration. Mech Dev
457 *127*, 321-328.
458 Grogg, M.W., Call, M.K., Okamoto, M., Vergara, M.N., Del Rio-Tsonis, K., and Tsonis,
459 P.A. (2005). BMP inhibition-driven regulation of six-3 underlies induction of
460 newt lens regeneration. Nature *438*, 858-862.
461 Guimond, J.C., Levesque, M., Michaud, P.L., Berdugo, J., Finnson, K., Philip, A., and
462 Roy, S. (2010). BMP-2 functions independently of SHH signaling and triggers cell
463 condensation and apoptosis in regenerating axolotl limbs. BMC Dev Biol *10*, 15.
464 Holley, S.A., Neul, J.L., Attisano, L., Wrana, J.L., Sasai, Y., O'Connor, M.B., De
465 Robertis, E.M., and Ferguson, E.L. (1996). The Xenopus dorsalizing factor noggin
466 ventralizes Drosophila embryos by preventing DPP from activating its receptor.
467 Cell *86*, 607-617.
468 Imokawa, Y., and Brockes, J.P. (2003). Selective activation of thrombin is a critical
469 determinant for vertebrate lens regeneration. Curr Biol *13*, 877-881.
470 Israel, D.I., Nove, J., Kerns, K.M., Kaufman, R.J., Rosen, V., Cox, K.A., and Wozney,
471 J.M. (1996). Heterodimeric bone morphogenetic proteins show enhanced activity
472 in vitro and in vivo. Growth Factors *13*, 291-300.
473 Jopling, C., Sleep, E., Raya, M., Marti, M., Raya, A., and Belmonte, J.C. (2010).
474 Zebrafish heart regeneration occurs by cardiomyocyte dedifferentiation and
475 proliferation. Nature *464*, 606-609.
476 Kikuchi, K., Holdway, J.E., Werdich, A.A., Anderson, R.M., Fang, Y., Egnaczyk, G.F.,
477 Evans, T., Macrae, C.A., Stainier, D.Y., and Poss, K.D. (2010). Primary contribution
478 to zebrafish heart regeneration by gata4(+) cardiomyocytes. Nature *464*, 601-
479 605.
480 Knapp, D., Schulz, H., Rascon, C.A., Volkmer, M., Scholz, J., Nacu, E., Le, M.,
481 Novozhilov, S., Tazaki, A., Protze, S., et al. (2013). Comparative transcriptional
482 profiling of the axolotl limb identifies a tripartite regeneration-specific gene
483 program. PLoS One *8*, e61352.
484 Kochegarov, A., Moses-Arms, A., M.C., H., and Lemanski, L.F. (2015). Identification
485 of Genes Involved in Limb Regeneration in the Axolotl Ambystoma mexicanum.
486 JSM Regenerative Medicine & Bioengineering *3*.
487 Kondo, T., and Raff, M. (2000). Oligodendrocyte precursor cells reprogrammed to
488 become multipotential CNS stem cells. Science *289*, 1754-1757.
489 Korchynskyi, O., and ten Dijke, P. (2002). Identification and functional
490 characterization of distinct critically important bone morphogenetic protein-
491 specific response elements in the Id1 promoter. J Biol Chem *277*, 4883-4891.

492 Lin, G., and Slack, J.M. (2008). Requirement for Wnt and FGF signaling in Xenopus
493 tadpole tail regeneration. Dev Biol *316*, 323-335.
494 Liu F, Ventura F, Doody J, Massague J.(1995). Human type II receptor for bone
495 morphogenic proteins (BMPs): extension of the two-kinase receptor model to
496 the BMPs. Mol Cell Biol *7*, 3479-86
497 Magaud JP, Sargent I, Mason DY. (1988). Detection of human white cell
498 proliferative responses by immunoenzymatic measurement of
499 bromodeoxyuridine uptake. J Immunol Methods. *106*, 95-100.
500 Makanae, A., Mitogawa, K., and Satoh, A. (2014). Co-operative Bmp- and Fgf-
501 signaling inputs convert skin wound healing to limb formation in urodele
502 amphibians. Dev Biol *396*, 57-66.
503 Mattler, L.E., and Bang, N.U. (1977). Serine protease specificity for peptide
504 chromogenic substrates. Thromb Haemost *38*, 776-792.
505 Nacu E, Gromberg E, Oliveira CR, Drechsel D, Tanaka EM. (2016). FGF8 and SHH
506 substitute for anterior-posterior tissue interactions to induce limb regeneration.
507 Nature. *533*, 407-10.
508 Okada, T.S. (1991). Transdifferentiation : flexibility in cell differentiation. (Oxford
509 Oxford ; New York: Clarendon Press ;
510 Oxford University Press).
511 Park, M.C., Park, Y.B., and Lee, S.K. (2008). Relationship of bone morphogenetic
512 proteins to disease activity and radiographic damage in patients with ankylosing
513 spondylitis. Scand J Rheumatol *37*, 200-204.
514 Poss, K.D. (2010). Advances in understanding tissue regenerative capacity and
515 mechanisms in animals. Nat Rev Genet *11*, 710-722.
516 Powers, J.C., Asgian, J.L., Ekici, O.D., and James, K.E. (2002). Irreversible inhibitors
517 of serine, cysteine, and threonine proteases. Chemical reviews *102*, 4639-4750.
518 Roedel, E.K., Schwarz, E., and Kanse, S.M. (2013). The factor VII-activating
519 protease (FSAP) enhances the activity of bone morphogenetic protein-2 (BMP-2).
520 J Biol Chem *288*, 7193-7203.
521 Ruppert, R., Hoffmann, E., and Sebald, W. (1996). Human bone morphogenetic
522 protein 2 contains a heparin-binding site which modifies its biological activity.
523 Eur J Biochem *237*, 295-302.
524 Ryan, T.J., Fenton, J.W., 2nd, Chang, T., and Feinman, R.D. (1976). Specificity of
525 thrombin: evidence for selectivity in acylation rather than binding for p-
526 nitrophenyl alpha-amino-p-toluate. Biochemistry *15*, 1337-1341.
527 Sandoval-Guzman, T., Wang, H., Khattak, S., Schuez, M., Roensch, K., Nacu, E.,
528 Tazaki, A., Joven, A., Tanaka, E.M., and Simon, A. (2014). Fundamental Differences
529 in Dedifferentiation and Stem Cell Recruitment during Skeletal Muscle
530 Regeneration in Two Salamander Species. Cell Stem Cell *14*, 174-187.
531 Straube, W.L. Brockes, J.P., Drechsel, D.N., Tanaka, E.M. (2004). Plasticity and
532 reprogramming of differentiated cells in amphibian regeneration: partial
533 purification of the serum factor that triggers cell cycle re-entry in differentiated
534 muscle cells. Cloning and Stem Cells *6*, 333-344
535 Sugiura, T., Wang, H., Barsacchi, R., Simon, A., and Tanaka, E.M. (2016). MARCKS-
536 like protein is an initiating molecule in axolotl appendage regeneration. Nature
537 *531*, 237-240.
538 Tacke, F., Gabele, E., Bataille, F., Schwabe, R.F., Hellerbrand, C., Klebl, F., Straub,
539 R.H., Luedde, T., Manns, M.P., Trautwein, C., et al. (2007). Bone morphogenetic

protein 7 is elevated in patients with chronic liver disease and exerts fibrogenic effects on human hepatic stellate cells. Dig Dis Sci *52*, 3404-3415.
Tanaka, E.M., Drechsel, D.N., and Brockes, J.P. (1999). Thrombin regulates S-phase re-entry by cultured newt myotubes. Curr Biol *9*, 792-799.
Tanaka, E.M., Gann, A.A., Gates, P.B., and Brockes, J.P. (1997). Newt myotubes reenter the cell cycle by phosphorylation of the retinoblastoma protein. J Cell Biol *136*, 155-165.
Uludag, H., Gao, T., Porter, T.J., Friess, W., and Wozney, J.M. (2001). Delivery systems for BMPs: factors contributing to protein retention at an application site. The Journal of bone and joint surgery. American volume *83-A Suppl 1*, S128-135.
Vindigni, A. (1999). Energetic dissection of specificity in serine proteases. Comb Chem High Throughput Screen *2*, 139-153.
Wang, H., Loof, S., Borg, P., Nader, G.A., Blau, H.M., and Simon, A. (2015). Turning terminally differentiated skeletal muscle cells into regenerative progenitors. Nature communications *6*, 7916.
Webster C, Silberstein L, Hays AP, Blau HM. (1988). Fast muscle fibers are preferentially affected in Duchenne muscular dystrophy. Cell. *52*, 503-13.
Wendling, D., Cedoz, J.P., Racadot, E., and Dumoulin, G. (2007). Serum IL-17, BMP-7, and bone turnover markers in patients with ankylosing spondylitis. Joint Bone Spine *74*, 304-305.
Ying, Q.L., Nichols, J., Chambers, I., and Smith, A. (2003). BMP induction of Id proteins suppresses differentiation and sustains embryonic stem cell self-renewal in collaboration with STAT3. Cell *115*, 281-292.
Zimmerman, L.B., De Jesus-Escobar, J.M., and Harland, R.M. (1996). The Spemann organizer signal noggin binds and inactivates bone morphogenetic protein 4. Cell *86*, 599-606.
Zou H, Wieder R, Massague J, Niswander L. (1997). Distinct roles of type I bone morphogenetic protein receptors in the formation and differentiation of cartilage. Genes Dev. *11*, 2191-2203

FIGURE LEGENDS

Fig. 1. BMP4 containing dimers are necessary and sufficient for S-phase re-entry, but recombinant molecules are less potent than native BMP4s.
(A) Dose response curves for recombinant bovine BMP4/4, BMP7/7 and BMP4/7. Square, green: Serum-derived BMP4 (SPRF); diamond, pink: recombinant BMP4/7; triangle, blue: recBMP4/4; inverted triangle, red: recBMP7/7; circle, lilac: mixture of recBMP4/4 plus recBMP7/7. Data are presented as mean ± SEM (n = 3).
(B) Addition of Noggin-FC to BMPs or SPRF inhibits S-phase. Square, green: Serum-derived BMP4 (SPRF); circle, pink: recombinant BMP4/7 heterodimer. Data are presented as mean ± SEM (n = 3).
(C) Noggin-FC-mediated depletion of BMPs and recovery from eluate. SPRF was pre-incubated with ProteinG beads (SPRF, PrG bead dep.) then incubated with noggin-FC-linked beads (SPRF, noggin-FC + PrG bead dep.). Elution from bound beads in 1% SDS (noggin-FC eluate) results in recovery of activity. Data are presented as mean ± SEM (n = 9). Significance calculated by Student's t-test.
(D) Sample eluted from the noggin-FC precipitate using 1% SDS (noggin-FC eluate) was separated on non-reducing SDS-PAGE and protein recovered by electroelution from gel slices as indicated. Positive activity in bioassay is observed in the gel slice in the size range of 28-36 kD (gel slice 7). Data are presented as mean ± SEM (n = 3).
(E) Immunodepletion of BMP4 from serum fraction depletes activity and elution recovers activity. SPRF was first pre-incubated with ProteinG beads (SPRF, PrG bead dep.) then incubated with anti-BMP4 antibody-linked beads for immunodepletion (SPRF, αBMP4 + PrG bead dep.). Elution from bound beads at pH11.5 (αBMP4 eluate) results in recovery of activity. Data are presented as mean ± SEM (n = 9) (SPRF, PrG bead dep. and SPRF, αBMP4 + PrG bead dep.) and n = 54 (αBMP4 eluate)). (see also Table S1)

Fig. 2. Increased potency of recombinant BMP4/7 after thrombin and plasmin treatment.
(A) Dose response of untreated recombinant human BMP4/7 (circle, green, solid line) and after treatment with thrombin (inverted triangle, blue, dotted line) or plasmin (square, red, dashed line). Data are presented as mean ± SEM (n = 3).
(B) Plasmin enhances the potency of human BMPs. Recombinant hBMP2/2 (circle, green line), BMP4/4 (square, purple line) or BMP7/7 (triangle, pink line) were incubated with increasing levels of plasmin. Samples were assayed on newt myotubes. Data are presented as mean ± SEM (n = 3).
(C) Western blot analysis of hBMP samples before and after plasmin treatment. Lanes 1-4: rhBMP2: 0.48 ng, 0.24 ng, 0.12 ng, 0.06 ng; rhBMP4 and rhBMP7: 0.96ng, 0.48 ng, 0.24 ng, 0.12 ng
(D) Treatment of hBMP4/4 homodimer with plasmin and thrombin results in altered gel mobility on silver stained SDS-PAGE and loss of immunoreactivity in western blot. Thrombin treatment results in a single smaller BMP4 band. Treatment with plasmin yields multiple cleavages. Time in hours refers to time of incubation with protease. (see also Figure S2C-D).

Fig. 3. Inhibition of BMP signaling via expression of dominant negative BMP receptors inhibits cell cycle re-entry *in vitro* and *in vivo*.
(A) Cultured newt myotubes electroporated with expression plasmids for the three dominant negative BMP receptors (dnALK2, dnALK3, dnALK6) together with nucGFP or nucGFP alone as control were stimulated with recombinant hBMP4/7 and then assayed for BrdU incorporation. Data are presented as mean ± SEM (n = 9 and n = 15 in control and dnBMPR respectively). Significance calculated by Student's t-test.
(B) Schematic outline of the *in vivo* experiments. Dotted lines indicate the cross sections for immunostaining. Representative staining pictures from a dnALK6 overexpressed limb are shown in (C) and (D).
(C) YFP^+ nuclei are MHC^+ and EdU^- in the stump muscle.
(D) Dedifferentiated YFP^+ nuclei in the blastema lose MHC and a fraction incorporates EdU. Arrows point to YFP^+EdU^- cells. Arrowheads point to YFP^+EdU^+ cells.
(E) Overexpression of dnALKs in myofibers reduces the cell cycle entry of the dedifferentiated cells during limb regeneration. Data are presented as mean ± SEM (n = 4). Significance calculated by Student's t-test.

Fig. 4. Molecular analysis of BMP signaling events in vitro and in vivo
(A) Luciferase activity assay of Smad-reporter in A1 newt myotube cultures. Data are presented as mean ± SEM (n=8). Significance calculated by Student's t-test.
(B) Luciferase reporter assay indicates increased SMAD signaling *in vivo* during the dedifferentiation stage of limb regeneration. The Smad-reporter and the Renilla luciferase control plasmids were electroporated into the uninjured newt limb, 5dpa and 11dpa blastemas. The luciferase activity was analyzed the next day. Data are presented as mean ± SEM (n=5). Significance calculated by Student's t-test.
(C) Dedifferentiating muscle cells display nuclearly localized phosphoSMAD. Immunohistochemical detection of increased phospho-smad1/5/8 in blastema nuclei compared to the stump (top of left panel). White line marks the amputation plane. Arrow indicates the stump region with low level of pSMAD. Asterisk indicates the background fluorescence of the myofibers.
Inset (right) de-differentiating YFP-expressing myofibre progeny (green) have $pSMAD^+$ nuclei (red). Arrowheads,YFP^+pSMAD^+ cells in the blastema. Scale bars, 200 µm (overview) and 20 µm (insert).
(D) Recombinant ΔN-BMP4 is more potent in inducing cell cycle reentry in cultured myotubes compared to full-length BMP4. FCS treatment was used as a positive control. Data are presented as mean ± SEM (n = 3 in control and 6 in all the other treatments). Significance calculated by Student's t-test.
(E) Schematic representation of the experiment testing the potency of the ΔN-BMP4 during limb regeneration. Equal amounts of baculovirus expressing full length BMP4, ΔN-BMP4 or cherry was injected into the early blastema. Muscle cell proliferation was quantified by MCM2 staining in the YFP+ myofibre progeny at 13 dpa.
(F) Dedifferentiated YFP^+ nuclei in the blastema proliferate. Arrows point to YFP^+MCM2^- cells. Arrowheads point to YFP^+MCM2^+ cells.

Formatted: English (U.S.)
Formatted: English (U.S.)
Formatted: English (U.S.)

(G) Both full length BMP4 and ΔN-BMP4 increase the fraction of proliferating myofibre derived cells but ΔN-BMP4 is more potent compared to full-length BMP4. Data are presented as mean ± SEM (n = 8). Significance calculated by Student's t-test.

EXPERIMENTAL PROCEDURES

CONTACT FOR REAGENT AND RESOURCE SHARING:

Further information and requests for resources and reagents should be directed to and will be fulfilled by the Lead Contact, Elly Tanaka (elly.tanaka@imp.ac.at)

EXPERIMENTAL MODEL AND SUBJECT DETAILS:

Red-spotted newts, *Notophthalmus viridescens*, were supplied by Charles D. Sullivan Co. (Nashville, TN, USA). Animals were kept in tanks fill with tap water at density of 4 animals/0.01m^2 and kept at 18-20°C with regular water change. Aquaria contained environmental enrichments composed of ceramic pieces for hiding and artificial plants. Animals were fed with frozen blood worms. Unsexed animals were randomly assigned to experimental groups.

Cell line, from *Notophthalmus viridescens*, called the A1 cell line was passaged and differentiated as described in Tanaka et al 1997. Newt myoblasts were cultured in 62.5% MEM (Invitrogen), 10% fetal bovine serum (Perbio), penicillin/streptomycin (Gibco) and glutamine (Gibco) on gelatin (Sigma) coated dishes, at 25°C and 2% CO_2. Cells were trypsinized once per week and split 1:3 before plating on flasks (Corning or Nunc) coated with 0.75% porcine gelatin Sex unknown. Cells not authenticated.

Human HEK293 cell line: Shaking cultures were maintained at 37°C, 8% CO_2 in Freestyle293 serum-free medium (Thermo Fischer). Sex: female. Cells purchased and not further validated in the laboratory.

Sf9 Cell line for baculovirus production: We used expresSF+ Cells (ProteinSciences (Meriden, CT, USA), sex: unknown. BV recombinants were

generated upon co-transfection of linearized bacmid DNA and a rescue vector using expresSF+ cell line (Protein Sciences Corp.). Cultured cells were maintained under continuous rotation suspension culture at 25˚C in ESF 921 Insect Cell Culture Medium (96-001, Expression Systems). Virions were subjected to two rounds of amplification previous to a final expansion, where 500 ml of expresSF+ cells at 0.6x10^6 cells/ml were infected with 500 µl of BV virion-containing supernatant. This final incubation proceeded for 4 days at 25˚C under continuous rotation, after which baculovirus particles were concentrated and purified using a gradient separation method.

METHOD DETAILS

Purification/Chromatography.

Crude bovine thrombin (Celliance Corp) was reconstituted at 20 mg/ml in 20 mM cation buffer (6.6 mM HEPES, 6.6 mM MES, 6.6 mM NaAcetate (pH 6.5) and loaded onto a HiTrap CMFF column. The flow through was collected and remaining thrombin inhibited with D-Phe-Pro-Arg-chloromethylketone, HCL (PPACK, Calbiochem). The flow through was mixed with phosphate buffer (pH 7.0) and ammonium sulfate to a final concentration of 33.3 mM and 100 mM respectively and loaded onto a HiTrap ButylFF column. Bound proteins were eluted in 50 mM phosphate buffer pH 7.0 by a stepwise gradient of 10 CV 100 mM ammonium sulfate, 0 mM ammonium sulfate, 20% Ethanol and 40% Ethanol.

The fraction eluted at 20% Ethanol (Butyl20) was mixed with NaCl to a final concentration of 200 mM and loaded onto a HiTrap Heparin column. Bound protein was eluted with a linear gradient of NaCl (0 mM to 1000 mM). Fractions

eluted between 430 mM and 680 mM NaCl were pooled, concentrated by ultrafiltration (MWCO 30,000) and mixed with CAPS (pH 11) to a final concentration of 100 mM. After incubation at room temperature for 4 hours the material was applied to a Superdex 200 column and fractions were collected.

Immunoprecipitation.

As a starting point for the immunoprecipitation a fraction of an intermediate step of the purification was used (Butyl20). Butyl20 was concentrated and dialyzed into 1X PBS. In order to remove IgG, the material was incubated with ProteinG beads at room temperature for 1 hour. Beads were removed and Butyl20-ΔIgG was incubated at 4°C, overnight with a) Noggin-FC or b) anti-BMP4 antibody (goat, polyclonal, R&D) or c) anti-EGFP antibody (goat, polyclonal, P.E.P.) that had been linked covalently to ProteinG beads. The beads were harvested and washed with a) 1X PBS, 0.01% SDS or b)/c) 10 mM phosphate buffer (pH8). Bound proteins were eluted with a) a step gradient of 0.1% SDS, 0.5% SDS, 1% SDS in 1X PBS or b)/c) 100 mM Phosphate buffer (pH11.5), 10 µg/ml aprotinin, for neutralization phosphate buffer (pH6.8) was added to a final concentration of 100 mM

Preparative SDS-PAGE.

The concentrated eluate that was obtained from immunoprecipitation was mixed with 5X sample buffer w/o DTT, incubated at 37°C for 1 hour and loaded onto a 4%-20% Tris-Glycine gradient gel (Anamed). Eletrophoresis was carried out at room temperature and 100 V in 1X SDS running buffer. Single gel slices were obtained and proteins were eluted using D-Tube dialyzer midi (Novagen). Elution was carried out in a horizontal electrophoresis chamber at room temperature, 100 V for 7 hours.

SDS-PAGE and western Blots.

Samples were mixed with 5X Sample Buffer (with or without DTT), incubated at 95°C for 5 min and loaded either onto 4%-20% Tris-Gycine gels (Anamed) or 12% Bis-Tris gels (NuPAGE). Electrophoresis was carried out either in 1X SDS running buffer or 1X MES-SDS running buffer (NuPAGE) at room temperature and 130 V. After blotting the membrane was blocked with 1X PBS, 2% BSA. Antibodies for western blot were reconstituted according to manufacture's advice and used at the following dilutions: BMP2 (rabbit, polyclonal, Acris antibodies) 1:1000, BMP4 (goat, polyclonal, R&D) 1:5000, BMP4 (goat, polyclonal, Santa Cruz) 1:1000, BMP5 (goat, polyclonal, R&D) 1:1000, BMP6 (goat, polyclonal, R&D) 1:1000, BMP7 (rabbit, polyclonal, Prepro Tech EC Ltd) 1:5000**.** As standards for western blot commercially available recombinant BMPs (R&D) were used.

De-glycosylation of samples.

Samples were denatured by adding SDS and DTT at a final concentration of 0.5 % and 20 mM respectively and subsequent heating to 95°C for 5 min. In the case of subsequent activity analyses the denaturing procedure was performed in the absence of DTT, at 37°C for 2 hours. After cooling to room temperature NP40 was added to a final concentration of 1%. The sample was mixed and 10X assay buffer (500 mM sodium phosphate, pH 7.5) was added to achieve a final concentration of 1X. The sample was then incubated with N-Glycosidase F (PNGase F) at a final concentration of 1200 U/ml (0.36 mg/ml) for 1 hour at 37°C.

Cell culture.

781 Newt myoblasts were cultured in 62.5% MEM (Invitrogen), 10% fetal bovine
782 serum (Perbio), penicillin/streptomycin (Gibco) and glutamine (Gibco) on
783 gelatine (Sigma) coated dishes, at 25°C and 2% CO_2. In order to induce myotube
784 formation, cells were placed into 0.5% serum medium for 5 to 6 days. Myotubes
785 were purified by sieving the trypsinized cell preparation through a 100 micron
786 mesh to remove large aggregates, then the flow-through was passed through a
787 35 micron mesh, which passed the contaminating mononucleates through but
788 trapped the myotubes. The myotubes were washed off of the sieves and plated
789 in 0.5% serum media on fibronectin coated 96-well plates (Tanaka, 1997).
790 Protein fractions usually in the presence of 0.5% serum medium were added to
791 cells 8 hours after cell preparation. Four days after adding of samples, cells were
792 labeled with bromodeoxyuridine (BrdU, Sigma) at a final concentration of 13
793 ug/ml. After 12 hours of labeling, cells were fixed and stained for BrDU as well as
794 the muscle marker myosin heavy chain (MHC) as described previously (Tanaka
795 et al., 1999). The percentage of $MHC^+/BrdU^+$ myotubes out of total MHC^+
796 myotubes was determined using an Axioplan 2 imaging microscope (ZEISS). The
797 specific activity of SPRF was defined in Units where the amount of material
798 added to myotubes that resulted in a 1% $BrdU^+$ myotube response in 150 µl of
799 culture media. In other words, if we added an amount of serum preparation of 10
800 µg protein /150 µl media that induced 10% of myotubes to take up BrdU, we
801 defined this as 1U SPRF/1µg protein added.
802 **Electroporation of newt myotubes**.
803 Newt myotubes from one cell culture dish (100 mm diameter) were harvested as
804 previously described (Tanaka et al., 1997). Cells were centrifuged (300 g, 3 min).
805 The cell pellet was re-suspended in 300 µl ice-cold 1X Steinberg's buffer and

transferred into a BTX electroporation device (pre-cooled to 4°C). 10 ug DNA were added per sample. The electroporation was carried out using a square pulse electroporator (BTX 830 Squarporator) at 75 V, 35 msec, for five pulses. 0.5% serum medium was added, myotubes were purified as described (Tanaka et al., 1997) and plated on fibronectin coated 96-well plates.

Cloning of BMP and noggin-FC constructs.

Complete human cDNAs for human BMP4, human BMP7 and human Noggin were obtained from the German Resource Center for Genome Research (RZPD). The coding sequence of noggin was inserted into pSUPER-M1, a derivative of Signal pIG-plus (R&D Systems) and p23 (a kind gift from Barbara Borgonovo) to generate a CMV promoter driven construct expressing a C-terminal human IgG1 Fc domain fusion. Human BMP4 and BMP7 were sub-cloned into pCMV-M2, a derivative of pCMVSport6 (Invitrogen). The bovine orthologs of human BMP4 and BMP7, human BMP4_S298P and human BMP7_S295G_M315V, as well as the human ΔN-BMP4 muntant (lacking residues K3 to K14 of mature human BMP4) were generated by site-directed mutagenesis using an overlap PCR protocol. All constructs were verified by sequencing.

Cloning of dnAlk constructs.

Mutations for Alk2, 3, 6: dnAlk2 K235R, dnAlk3 K261R, dnAlk6 K231R.

Human Alk2, 3, 6 cDNAs were obtained from RZPD (now CellBioSource) and coding sequences were PCR amplified to incorporate point mutants by standard methods. PCR products were digested with NheI & EcoRI and ligated, transformed in DH5alpha. A Caggs-GFP vector was digested with NheI & EcoRI and dnAlk sequences were inserted by ligation.

Generation of the SceI-mTol2-Caggs-lpCherry-H2B-YFP-T2A-dnAlk constructs.

831 The control plasmid (SceI-mTol2-Caggs-lpCherry-H2B-YFP-T2A-User) used in
832 ((Sandoval-Guzman et al., 2014) were digested with BbvCI.
833 Each dnAlk fragment was PCR amplified using Caggs-dnAlks for template and
834 assembled by Gibson assembly (NEB).
835 nucGFP was obtained from Clontech (eGFP-N2).
836 **Expression of recombinant proteins**
837 Recombinant proteins were expressed by transient transfection of suspension
838 cultures of HEK293 cells and secreted into the medium. For the expression of
839 BMP heterodimers expression constructs encoding the individual BMPs were co-
840 transfected into HEK293 cells. Shaking cultures were maintained at 37°C, 8%
841 CO_2 in Freestyle293 serum-free medium (Invitrogen). For transfection, plasmid
842 DNA:PEI complexes, preformed at 10 µg/mL DNA and 100 µg/mL PEI
843 (Polysciences, linear 25kD, #23966) in 150 mM NaCl were diluted 1:10 into cells
844 adjusted to 2 x 10^6/ml. After shaking incubation for 4 hours, the medium was
845 replaced and the cultures diluted to 1 x 10^6 cells/ml. After shaking for 4 days,
846 conditioned medium was harvested by centrifugation (500 x g, 5 min), sterile
847 filtered (0.2 µM), concentrated using Amicon Ultra-15 centrifugal filter units
848 (Millipore), and dialyzed into PBS. Bacterially expressed recombinant human
849 BMP4/4 used for mass spectrometry analysis was a kind gift from Walter Sebald.
850 Bacterially expressed recombinant human BMP4/4 and BMP4/7 used for Edman
851 sequencing were purchased from R&D.
852 **BMP Inhibition.**
853 The sample was mixed with noggin-FC or antibody and incubated at room
854 temperature for 1 hour before loading on myotubes.
855 **Plasmin/Thrombin Digest**.

If not stated differently the digests for cell assay samples was performed in 50 mM Tris, 150 mM NaCl, pH7.4 (plasmin) or 50 mM Tris, 150 mM NaCl pH8.3 (thrombin) buffer. Plasmin (Enzyme Research Labs) or thrombin (Enzyme Research Labs) were added to the sample at 16 ug/ml final concentration (molar ratio protease:BMP = 1:10) and incubated at 37°C for 4 hours. In order to inhibit proteolytic activity after incubation, PPACK was added to a final concentration of 4 µg/ml. As a quality control, before usage, the activity and specificity of plasmin and thrombin was shown by digesting their specific substrates, ChromozymPL and ChromozymTH (Boehringer-Mannheim) respectively. Plasmin digestion of bacterially expressed recombinant hBMP4/4 for mass spectrometry analysis was performed in 20 mM ammonium carbonate, 4 mM Hepes, 4 mM NaAcetate at 37°C for 15 minutes, 3 hours and 24 hours with a molar ratio of plasmin:BMP4/4 of 1:60.

Mass spectrometry.

Gel separated proteins were reduced, alkylated and in-gel digested with trypsin as described in (Shevchenko et al., 2006). After digestion, peptides were twice extracted with 50 µl of 5% formic acid and 50% acetonitrile, dried down, re-dissolved in 20 µL of 5 % (v/v) formic acid and analyzed by mass spectrometry.

LC-MS/MS analysis of peptide mixtures was carried out on an Ultimate nanoLC system (Dionex, Amsterdam, The Netherlands) interfaced on-line to a LTQ linear trap mass spectrometer (Thermo Fisher Scientific, San Jose) (Waridel et al., 2007). Acquired MS/MS spectra were searched against a comprehensive NCBI protein sequences database using MASCOT software (Matrix Science, v.2.2.0) installed on a local server under the following settings: mass tolerance was set as 2 Da for peptide masses and 0.5 Da for masses of peptide fragments; variable

modifications: Propionamide (C), Carbamidomethyl (C), N-acetylation (Protein N-terminus), Oxidation (M); enzyme: trypsin; two missed cleavages were allowed. All hits with peptide ions scores above 25 were manually evaluated.

MS analysis of plasmin treated bacterially produced recombinant hBMP4/4.

Plasmin digestion was performed in 10 mM Ammonium bicarbonate. One aliquot of the sample (5 µl) was acidified (1 µl 30% formic acid) and after addition of 20 µl of 80% acetonitrile solvent was evaporated in a speed vac (non-reduced sample). A second aliquot of the sample (5 µl) was acidified (1 µl 30% formic acid) to stop digestion, neutralized with ammonium bicarbonate and reduced with 10 mM DTT (2 hours at 37°C) and alkylated with 50 mM iodacetamide (1.5 hours at room temperature in the dark). Excess of iodacetamide was captured by a second addition of 10 mM DTT and further incubation for 1 hour at room temperature. After addition of 20 µl of 80% acetonitrile solvent was evaporated in a speed vac and dry samples were stored at -20°C until analysis. For HPLC-MS/MS analysis samples were separated in a linear gradient of water/acetonitrile with 0.1% formic acid on a 75 µm i.d. C-18 Acclaim capillary column (Dionex, Idstein, Germany) at a flow rate of 200 nl/min with an Eksigent 2D Nano-LC system (Eksigent, Dublin, CA, USA). The HPLC system was hyphenated via a TriVersa Nanomate automatic source (Advion, Ithaca, USA) to an Orbitrap-Velos mass spectrometer (Thermo Fisher Scientific, Bremen, Germany) operated in data-dependent acquisition mode with a nominal resolution of 60000 at 400 m/z and lock mass enabled for MS spectra and MS/MS acquisition in the Velos ion trap.

Animal procedures

Red-spotted newts, *Notophthalmus viridescens*, were supplied by Charles D. Sullivan Co. (Nashville, TN, USA). Plasmid preparation injection, and electroporation were carried out as in (Sandoval-Guzman et al., 2014). Animals were anesthetized in 0.1% ethyl 3-aminobenzoate methanesulfonate (Sigma) for 15 min. Forelimbs were amputated above the elbow, and the bone and soft tissue were trimmed to produce a flat amputation surface. Animals were left to recover overnight in an aqueous solution of 0.5% sulfamerazine (Sigma). At specified time-points, the regenerating limbs were collected. Three ul of 5mg/ml AEBSF (Roche) and/or baculo virus expressing BMP4 or cherry was injected into the blastema at 6dpa and 9dpa. For EdU-labelling, animals were injected intraperitoneally with 50-100 µl of 1mg/ml EdU. All surgical procedures were performed according to the European Community and local ethics committee guidelines.

Luciferase assay

Smad-luc reporter (pGL3-BRE-"BMP Responsive Element"-Luciferase plasmid) was from Addgene, pGL3-basic and pRL-Renilla were from Promega. Dual Luciferase Assay system (Promega) was used to measure the luciferase activity in A1 myotubes, and in limbs. An Amaxa Nucleofector was used for electroporation of A1 myoblasts (Program T30) and the myoblasts were differentiated into myotubes over 7 days. Recombinant BMP4/7 with or without noggin was added into the cultured myotubes (500ng/ml). A1 myotubes were lysed after 24h using the passive lysis buffer provided in the dual luciferase reporter assay kit following the manufacturer's instructions. The *in vivo* luciferase analysis procedures were modified from (Yun et al, 2013). In short, Smad-luc and pRL-Renilla plasmids were mixed at 10ug/ul. Three or 5 ul of

plasmid solutions were injected into blastemas or uninjured limbs, respectively. Electroporations were performed by NEPA21 electroporator with parallel fixed platinum electrodes using 10 pulses (duration: 100ms, voltage: 30volts decending). Tissues were collected 24h after electroporation and immediately homogenized in passive lysis buffer (Promega).Lysates were centrifuged to remove debris, and assayed according to the dual luciferase reporter protocol. The activities of the Smad-Luc reporter were normalized to the activity of the internal Renilla control and expressed as relative luciferase activity (Firefly/Renilla).

Formatted: English (U.S.)

Baculo virus production

Production of pseudotyped baculovirus was as described in Nacu et al 2016. Baculovirus was pseudotyped with vsv-ged gene, which was inserted into the rescue vector under the baculovirus polyhedrin promoter.BMP4 or Cherry constructs were cloned into a rescue vector using standard restriction enzyme methods, and are expressed under the control of a CMV promoter. The generation of baculoviruses was carried out by co-transfection of the above-mentioned rescue vector together with replication incompetent baculovirus DNA into SF9 ESF insect cell line. Upon culture expansion, recombinant baculovirus particles were collected, concentrated and purified using the sucrose gradient separation method. The titer was assessed in SF9ET cells, by means of end-point dilution assay.

Immunohistochemistry

Frozen sections (8 µm) were thawed at room temperature and fixed in 4% formaldehyde for 5 min. Sections were blocked with 5% donkey serum and 0.1% Triton-X for 30 min at room temperature. Sections were incubated with anti-GFP

(Abcam 6673) and anti-MHC (DSHB) or anti-Phospho-Smad1/5/8 (Cell Signaling 9511) overnight at 4°C and with secondary antibodies for 1 hour at room temperature. Antibodies were diluted in blocking buffer and sections were mounted in mounting medium (DakoCytomation) containing 5 µg/ml DAPI (Sigma). PhosSTOP (Roche) was used during Phospho-Smad1/5/8 staining process. EdU detection was performed according to (Salic and Mitchison, 2008). An LSM 700 Meta laser microscope with LSM 6.0 Image Browser software (Carl Zeiss) was used for confocal analyses. One in every 6 (Figure 3) or 10 (Figure 4) sections was selected and counted.

QUANTIFICATION AND STATISTICAL ANALYSIS

Error bars represent SEM unless otherwise indicated. Statistical analysis was performed using GraphPad Prism software.

Analysis of in vitro myotube cell cycle entry data:

The percentage of $BrdU^+$ myotubes were counted and always presented as mean±SEM from n samples. In Figure 1C the sample size was n = 9 samples for each condition. Each sample was derived from counting one separate well containing a median of 84 myotubes per well. In Figure 1E the sample size was n = 9 samples (SPRF, PrG bead dep. and SPRF, αBMP4 + PrG bead dep.) and n = 54 samples (αBMP4 eluate). Each sample was derived from counting one separate well containing a median

978 of 44 myotubes per well. In Figure 3A the sample size was n = 9 samples
979 (control) and n = 15 samples (dnBMPR). Each sample was derived from
980 counting one separate well containing a median of 41 myotubes per well.
981 In Figure 4D the sample size was n = 3 in control and n = 6 in other
982 treatments. Each sample was derived from counting of one separate well
983 containing a median of 132 myotubes. The statistical significance was
984 always analyzed by an unpaired, two-tailed Student's t-test, (95%
985 confidence intervals). Please refer to figures for p-values.
986
987 Analysis of immunofluorescence staining data:
988 The percentages of EdU^+/YFP^+ cells were counted and presented as
989 mean±SEM, n = 4 limbs (Figure 3E), 8 limbs (Figure 4G), 6 limbs in
990 PBS and 8 limbs in AEBSF (Figure S4B), 8 limbs (Figure S4C) per each
991 treatment group. The statistical significance was analyzed by Student's t-
992 test, (95% confidence intervals). Please refer to figures for p-values.
993
994 Analysis of luciferase activity data:
995 The in vitro luciferase activity data were presented as mean±SEM, n = 8
996 samples (Figure 4A). Each plate contained 10^6 cells and triplicate plates
997 were averaged for each sample. The in vivo luciferase activity data were
998 presented as mean±SEM, n = 5 limbs per each group (Figure 4B). The

statistical significance was analyzed by Student's t-test, (95% confidence intervals). Please refer to figures for p-values.

Figure 1

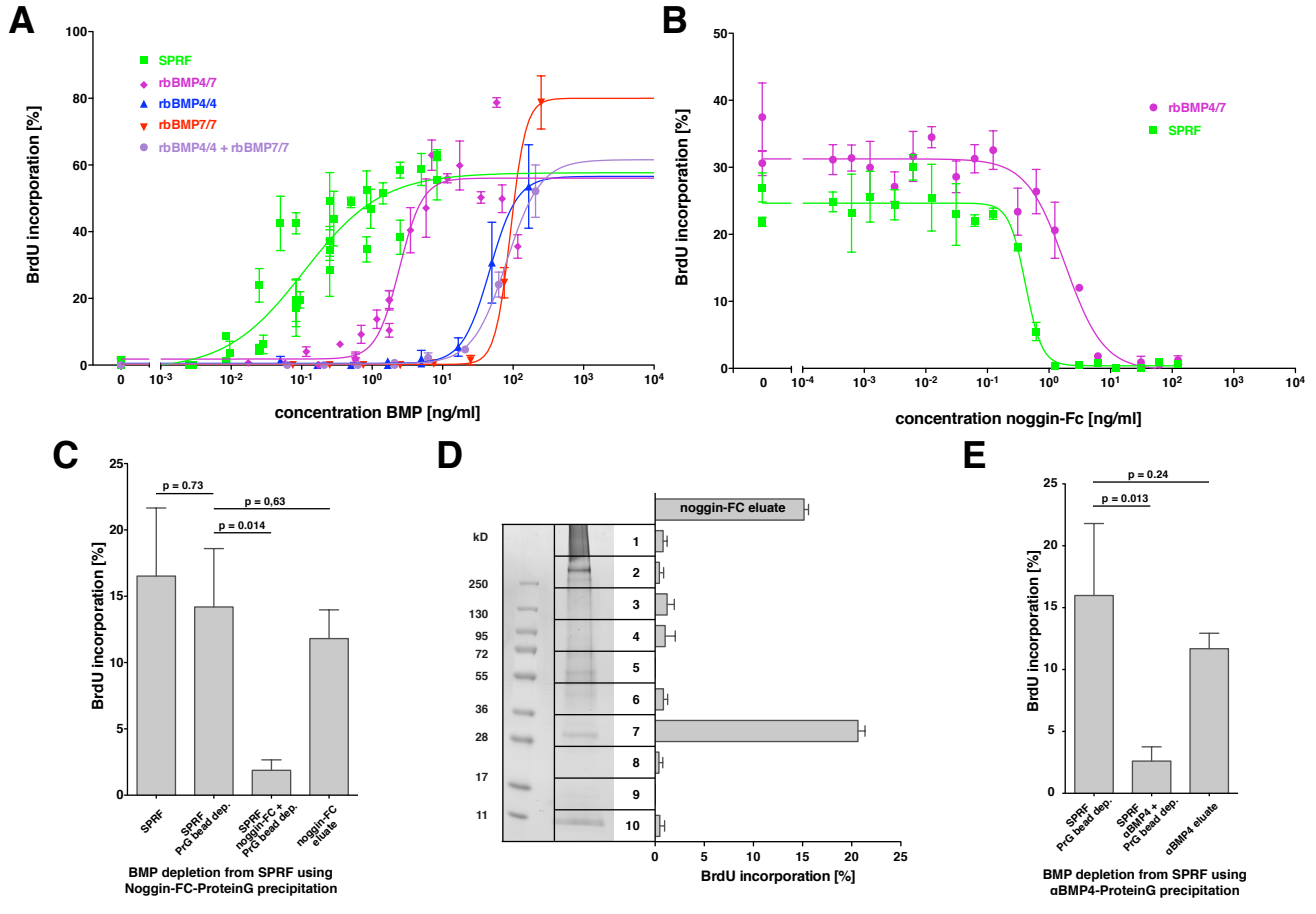
A
SPRF
rbBMP4/7
rbBMP4/4
rbBMP7/7
rbBMP4/4 + rbBMP7/7
BrdU incorporation [%]
concentration BMP [ng/ml]
B
rbBMP4/7
SPRF
BrdU incorporation [%]
concentration noggin-Fc [ng/ml]
C
p = 0.73
p = 0,63
p = 0.014
BrdU incorporation [%]
SPRF
SPRF PrG bead dep.
SPRF noggin-FC + PrG bead dep.
noggin-FC eluate
BMP depletion from SPRF using Noggin-FC-ProteinG precipitation
D
noggin-FC eluate
kD
250
130
95
72
55
36
28
17
11
1
2
3
4
5
6
7
8
9
10
BrdU incorporation [%]
E
p = 0.24
p = 0.013
BrdU incorporation [%]
SPRF PrG bead dep.
SPRF αBMP4 + PrG bead dep.
αBMP4 eluate
BMP depletion from SPRF using αBMP4-ProteinG precipitation

Figure 2

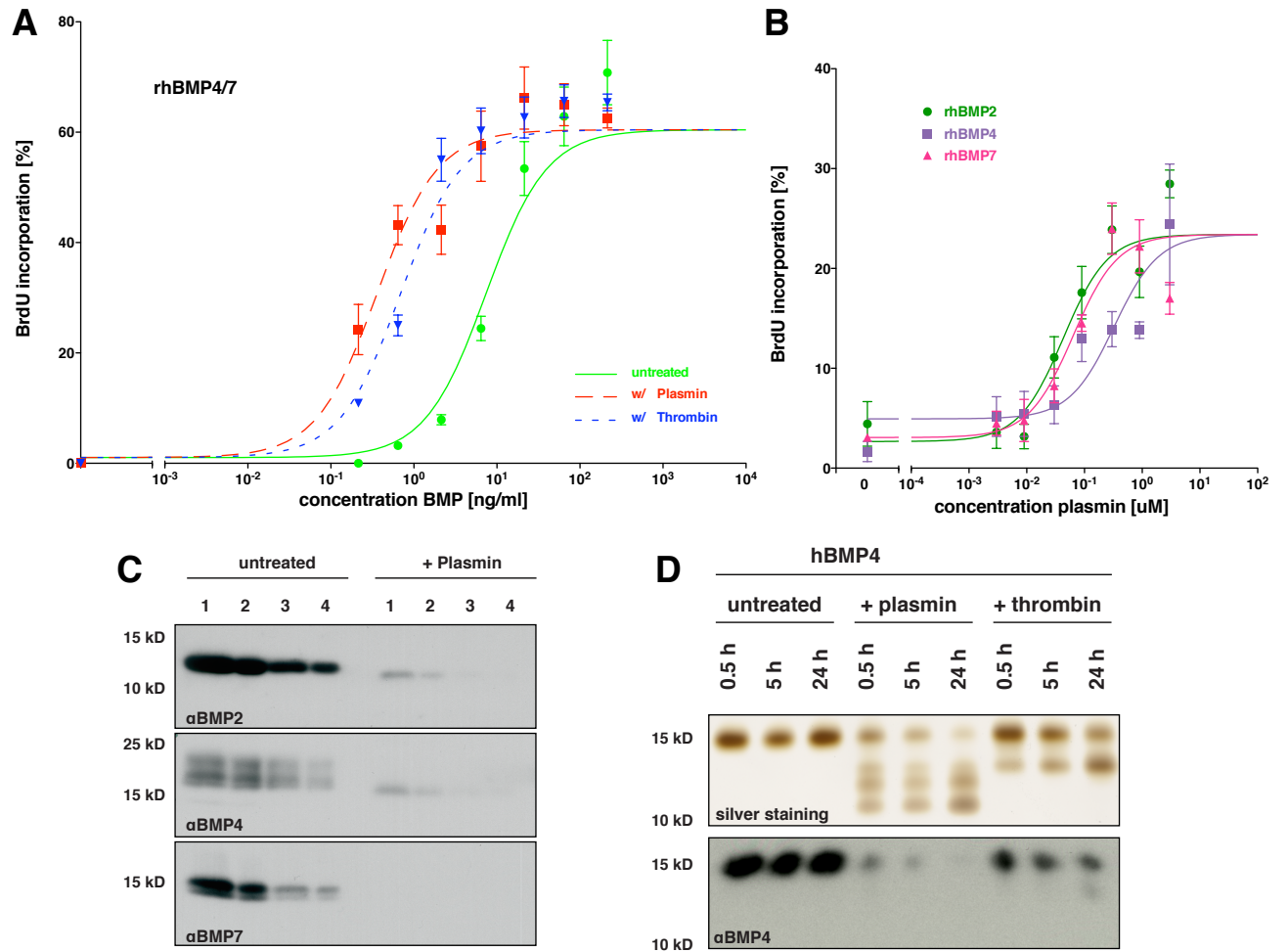
A
rhBMP4/7
BrdU incorporation [%]
concentration BMP [ng/ml]
untreated
w/ Plasmin
w/ Thrombin
B
rhBMP2
rhBMP4
rhBMP7
BrdU incorporation [%]
concentration plasmin [uM]
C
untreated
+ Plasmin
1 2 3 4 1 2 3 4
15 kD
10 kD
αBMP2
25 kD
15 kD
αBMP4
15 kD
αBMP7
D
hBMP4
untreated
+ plasmin
+ thrombin
0.5 h
5 h
24 h
15 kD
10 kD
silver staining
15 kD
10 kD
αBMP4

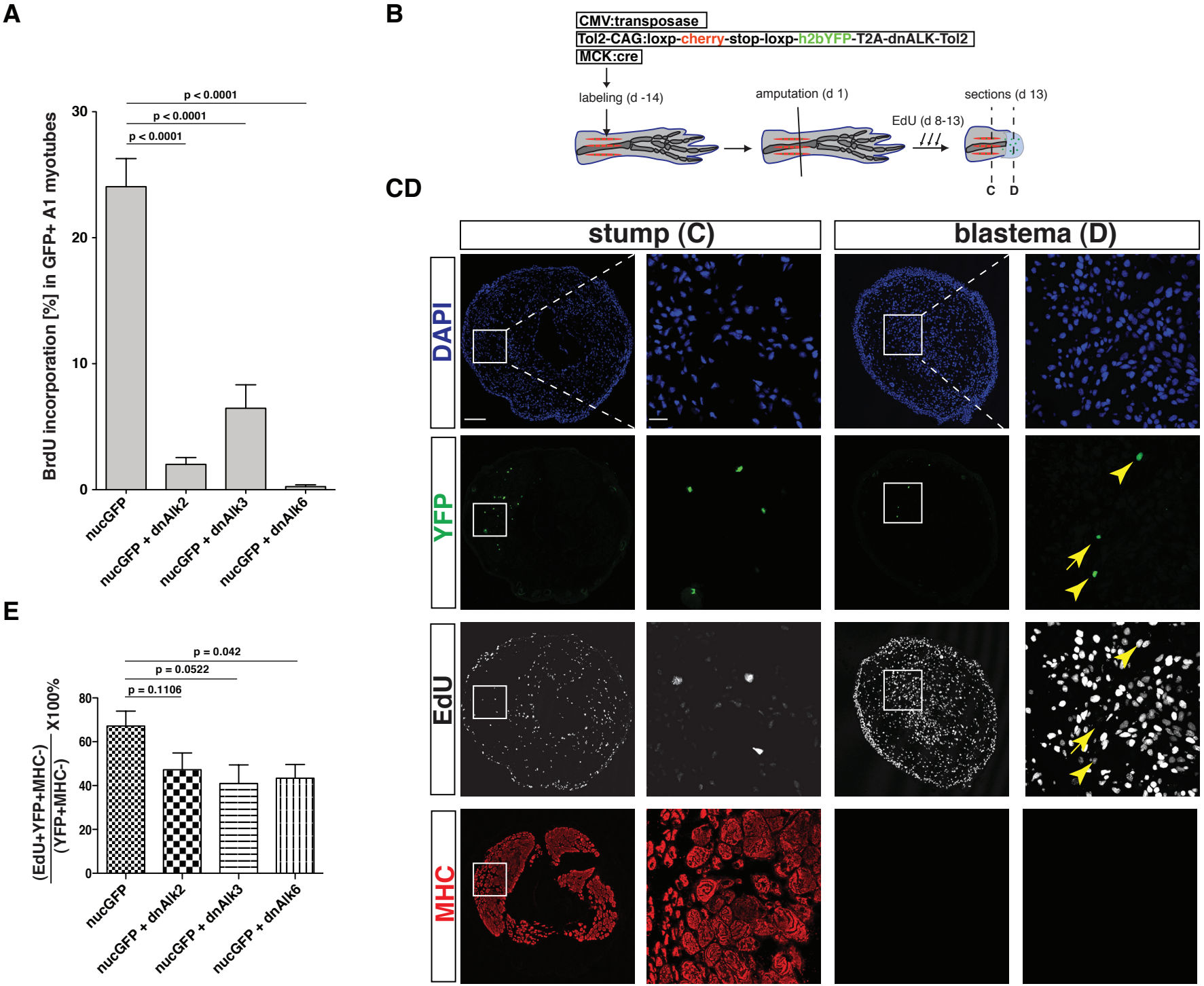
A
BrdU incorporation [%] in GFP+ A1 myotubes
p < 0.0001
p < 0.0001
p < 0.0001
30
20
10
0
nucGFP
nucGFP + dnAlk2
nucGFP + dnAlk3
nucGFP + dnAlk6
B
CMV:transposase
Tol2-CAG:loxp-cherry-stop-loxp-h2bYFP-T2A-dnALK-Tol2
MCK:cre
labeling (d -14)
amputation (d 1)
EdU (d 8-13)
sections (d 13)
C
D
CD
stump (C)
blastema (D)
DAPI
YFP
EdU
MHC
E
(EdU+YFP+MHC-) / (YFP+MHC-) X100%
p = 0.042
p = 0.0522
p = 0.1106
80
60
40
20
0
nucGFP
nucGFP + dnAlk2
nucGFP + dnAlk3
nucGFP + dnAlk6

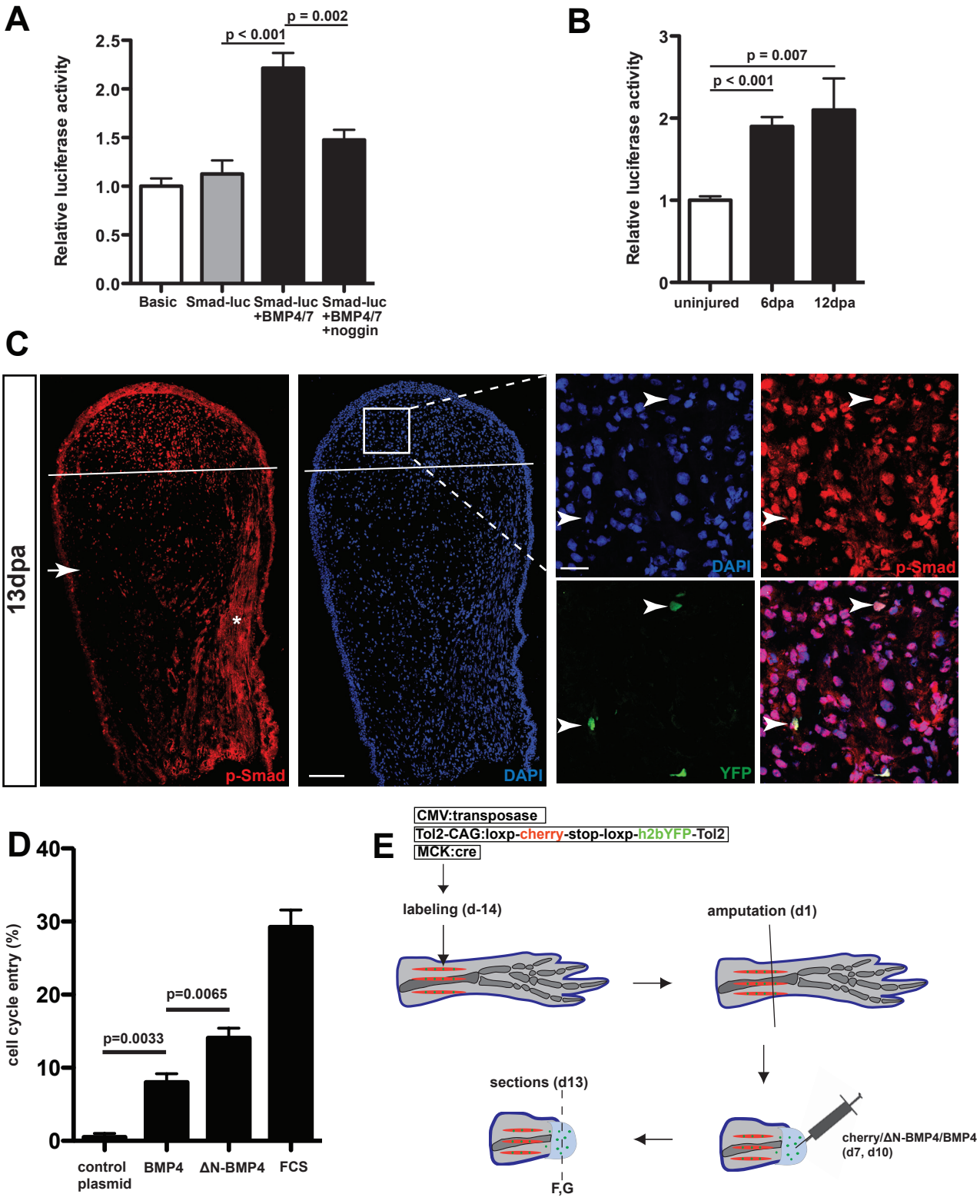
A
Relative luciferase activity
2.5
2.0
1.5
1.0
0.5
0.0
p < 0.001
p = 0.002
Basic
Smad-luc
Smad-luc +BMP4/7
Smad-luc +BMP4/7 +noggin
B
Relative luciferase activity
3
2
1
0
p = 0.007
p < 0.001
uninjured
6dpa
12dpa
C
13dpa
p-Smad
DAPI
DAPI
p-Smad
YFP
D
cell cycle entry (%)
40
30
20
10
0
p=0.0033
p=0.0065
control plasmid
BMP4
ΔN-BMP4
FCS
E
CMV:transposase
Tol2-CAG:loxp-cherry-stop-loxp-h2bYFP-Tol2
MCK:cre
labeling (d-14)
amputation (d1)
sections (d13)
F,G
cherry/ΔN-BMP4/BMP4 (d7, d10)
F
cherry (13dpa)
ΔN-BMP4 (13dpa)
YFP cherry DAPI
MCM2
G
cell cycle entry (%)
60
40
20
0
p=0.0005
p=0.0171
cherry
BMP4
ΔN-BMP4

Inventory of Supplemental Information

Supplemental Figures

Figure S1. Bovine BMP4 co-fractionates with serum-derived myotube S-phase re-entry inducing activity. Relates to Figure 1.

Figure S2. Serum BMPs are more potent than recombinant BMPs under serum-free conditions, BMP signaling is required for S-phase re-entry of newt myotubes and the potency of recombinant BMPs is increased after thrombin and plasmin treatment. Relates to Figure 1 and Figure 2.

Figure S3. Mapping the target sites for thrombin and plasmin in hBMP4/4 by Edman sequencing. Relates to Figure 2, Data S1 and Table S2.

Figure S4. Serine proteases act upstream of BMPs to promote cell cycle entry of dedifferentiating myofibers. Relates to Figure 4.

Supplemental Tables

Table S1. Bone morphogenetic proteins identified in BMP4 immunoprecipitation by mass spectrometry. Relates to Figure 2.

Supplemental Tables (separate .xlsx files)

Table S2. Edman sequencing of rhBMPs. Relates to Figure 2 Figure S3 and Data S1.

Table S3. Bovine BMP peptides identified by mass spectrometry. Relates to Figure 1 and Figure S1.

Supplemental Data (separate .pdf file)

Data S1. Traces of Edman sequencing of rhBMPs. Relates to Figure 2, Figure S3 and TableS2.

Supplemental Figures

Figure S1

A

Step	Chromatography	Yield (%)	Purification (fold)	BMP4 (ng/mg)
1	Crude Bovine Thrombin	100	20	not detectable
2	Cation Exchange (CMFF)	87	26	not detectable
3	Hydrophobic Interaction (Butyl20)	64	540	4.5
4	Heparin Affinity	15	5900	30
5	Gel Filtration	3.9	20000	200

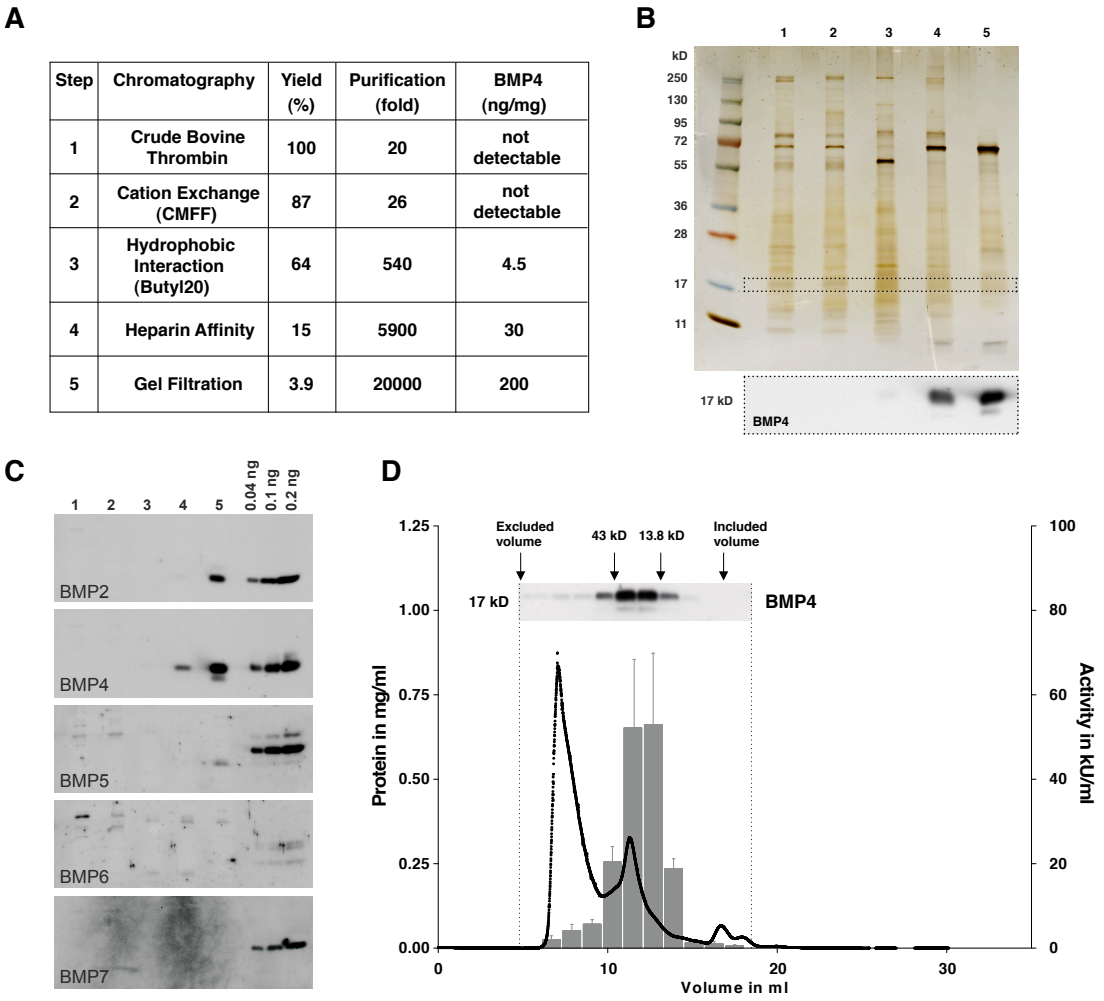

Figure S1. Bovine BMP4 co-fractionates with serum-derived myotube S-phase re-entry inducing activity. Relates to Figure 1.

(A) Summary of purification steps and –fold enrichment of activity across the purification. Specific activity of pooled peak fractions from each column step was measured as the described in Materials and Methods based on the myotube bioassay. The "fold purification" was calculated based on the fold increase in specific activity found in the peak pool from each chromatography step and "yield" was calculated based on the total amount of activity found in the peak pool from each step. BMP4 was quantitated by western blot using commercial recombinant hBMP4/4 as standard protein.

(B) Top: silver stained reducing gel of peak fractions from the five column steps listed in (A). Equal amount of protein were loaded in each sample. Dotted lines at 17

kD mark the region of the gel shown in the western blot below. Bottom: anti-BMP4 western blot of samples shows enrichment of BMP4 across the purification.
(C) The indicated BMPs were detected by western blotting. 1-5: peak activity fractions of single purification steps: (1) Crude Bovine Thrombin - starting material (2) Cation Exchange Chromatography (3) Hydrophobic Interaction Chromatography (4) Heparin Affinity Chromatography (5) Size Exclusion Chromatography. For each fraction 1 µg total protein was used in reducing conditions. 0.04 ng, 0.1 ng and 0.2 ng of respective BMP standards were loaded in control lanes.
(D) Co-fractionation of BMP4 with activity during gel filtration fractionation. Protein elution profile (black line), activity profile (gray bars), and BMP4 immunoblotting across the gel filtration column (purification step 5) shows that BMP4 co-fractionates with the activity. The elution volumes of protein standards are indicated at the top of the chart. Fractions that eluted within the markers for the excluded volume (blue dextran, 2000 kD) and the included volume (salt peak) were analyzed. Amongst others, ovalbumin (43 kD) and ribonuclease A (13.8 kD) were used as molecular weight standards. For western blotting, pools from three consecutive fractions were prepared and equal volumes of pooled fractions were separated by SDS-PAGE in reducing conditions. The S-phase re-entry activity for the pooled samples was calculated by averaging the activity that was found from individually assaying the single fractions of each pool on newt myotubes.

Figure S2

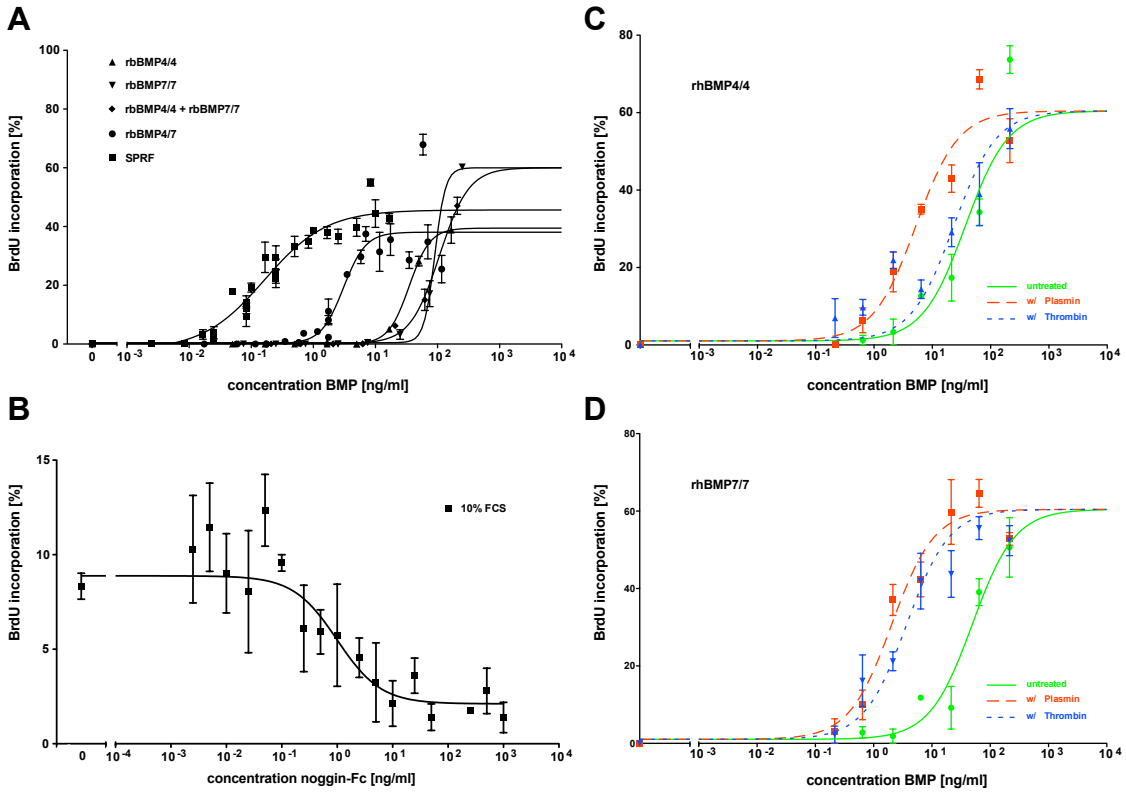

Figure S2. Serum BMPs are more potent than recombinant BMPs under serum-free conditions, BMP signaling is required for S-phase re-entry of newt myotubes and the potency of recombinant BMPs is increased after thrombin and plasmin treatment. Relates to Figure 1 and Figure 2.

(A) Dose response curves under serum-free conditions for recombinant bovine BMP4/4, BMP7/7 and BMP4/7 containing dimers produced by transfection of 293 cells compared to dose response for serum-derived bovine BMP4-containing dimers. BMP4 protein was quantitated by western blotting against a standard purified protein preparation. Square: Serum-derived BMP2 and BMP4 (SPRF), Circle: recombinant BMP4/7 heterodimer, Diamond: recBMP4/4 plus recBMP7/7 mixture, Inverted triangle: recBMP7/7, Triangle: recBMP4/4. Data are presented as mean ± SEM (n = 3).

(B) Noggin inhibits the S-phase re-entry activity in fetal calf serum (FCS). Inhibition of S-phase re-entry by addition of recombinant human noggin-Fc, produced by transfection of HEK293 cells, to FCS. Data are presented as mean ± SEM (n = 3).

(C) Dose response of untreated recombinant human BMP4/4 homodimer (circle, green, solid line) and after treatment with thrombin (triangle, blue, dotted line) or plasmin (square, red, dashed line). Data are presented as mean ± SEM (n = 3).

(D) Dose response of untreated recombinant human BMP7/7 homodimer (circle, green, solid line) and after treatment with thrombin (inverted triangle, blue, dotted

line) or plasmin (square, red, dashed line). BMPs are made in HEK293 cells. Data are presented as mean ± SEM (n = 3).

Figure S3

A

```
hBMP4      --SPKHHSQRARKKNKN--------------------CRRHSLYVDFSDVGWNDWIVAPPGYQAFYCHG    47
hBMP7      STGSKQRSQNRSKTPKNQEALRMANVAENSSSDQRQACKKHELYVSFRDLGWQDWIIAPEGYAAYYCEG    69
             ..*::**.  *. **                    *::*.***.* *:**:***:** ** *:**.*

hBMP4      DCPFPLADHLNSTNHAIVQTLVNSVN-SSIPKACCVPTELSAISMLYLDEYDKVVLKNYQEMVVEGCGCR  116
hBMP7      ECAFPLNSYMNATNHAIVQTLVHFINPETVPKPCCAPTQLNAISVLYFDDSSNVILKKYRNMVVRACGCH  139
           :*.*** .::*:**********: :* .::**.**.**:*.***:**:*: .:*:**:*::***..***:
```

B

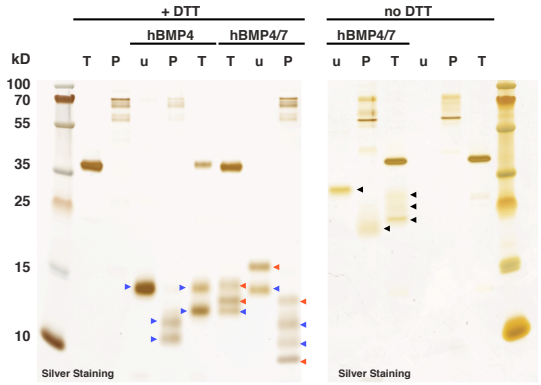

C

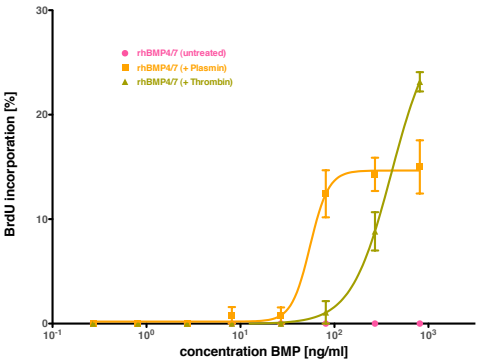

D

```
mathBMP5       -AANKRKNQNRNKSSSHQDSSRMSSVGDYNTSEQKQACKKHELYVSFRDLGWQDWIIAPE 59
mathBMP6       SASSRRRQQSRNRSTQSQDVARVSSASDYNSSELKTACRKHELYVSFQDLGWQDWIIAPK 60
mathBMP7       STGSKQRSQNRSKTPKNQEALRMANVAENSSSDQRQACKKHELYVSFRDLGWQDWIIAPE 60
mathBMP2       --QAKHKQRKRLKS----------------------SCKRHPLYVDFSDVGWNDWIVAPP 36
mathBMP4       -SPKHHSQRARKKNK----------------------NCRRHSLYVDFSDVGWNDWIVAPP 38
                   :: .: * :.                        *::* ***.* *:**:***:**

mathBMP5       GYAAFYCDGECSFPLNAHMNATNHAIVQTLVHLMFPDHVPKPCCAPTKLNAISVLYFDDS 119
mathBMP6       GYAANYCDGECSFPLNAHMNATNHAIVQTLVHLMNPEYVPKPCCAPTKLNAISVLYFDDN 120
mathBMP7       GYAAYYCEGECAFPLNSYMNATNHAIVQTLVHFINPETVPKPCCAPTQLNAISVLYFDDS 120
mathBMP2       GYHAFYCHGECPFPLADHLNSTNHAIVQTLVNSVN-SKIPKACCVPTELSAISMLYLDEN 95
mathBMP4       GYQAFYCHGDCPFPLADHLNSTNHAIVQTLVNSVN-SSIPKACCVPTELSAISMLYLDEY 97
               ** * **.*:*.***  ::*:**********: :  . :**.**.**:*.***:**:*:

mathBMP5       SNVILKKYRNMVVRSCGCH 138
mathBMP6       SNVILKKYRNMVVRACGCH 139
mathBMP7       SNVILKKYRNMVVRACGCH 139
mathBMP2       EKVVLKNYQDMVVEGCGCR 114
mathBMP4       DKVVLKNYQEMVVEGCGCR 116
               .:*:**:*::***..***:
```

E

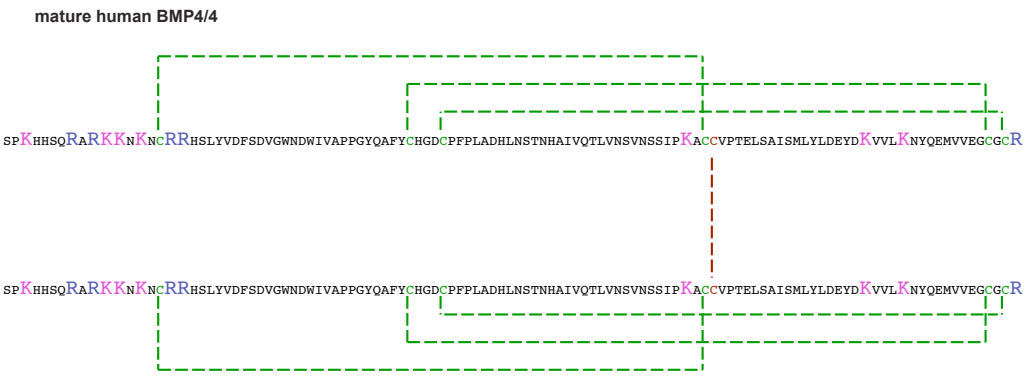

Figure S3. Mapping the target sites for thrombin and plasmin in hBMP4/4 by Edman. Relates to Figure 2, Data S1 and Table S2.

(A) N-terminal peptides found along the BMP4 and BMP7 sequences after Edman degradation analysis of BMP4/4 and BMP4/7. The N-terminus of untreated hBMP4/4 was verified in reducing conditions (pink - SPKHH). Thrombin-treated hBMP4/4 homodimer in the presence of DTT detected one main sequence ARKKN (green) suggesting cleavage at R8. The plasmin treated BMP4/4 yielded two major N-termini, KKNKN and NYQEMVV. In the plasmin treated hBMP4/7 heterodimer five main sequences (orange) NYQEMVV and KKNKNCR, as well as MANVAEN, DLGWQDW and NMVVRAC were found, indicating that plasmin targets hBMP4 at R10 and K103, whereas BMP7 is targeted at R22, R48 and R129.

(B) Samples from panel (C) were applied to SDS-PAGE in the presence or absence of DTT. For identification of hBMP4 versus hBMP7 peptides in hBMP4/7-derived samples, hBMP4/4 - untreated or after protease treatment - was run as a size standard in reducing conditions. Arrows indicate hBMP peptides (black = hBMP4/7 heterodimer peptides, blue = hBMP4 monomeric peptides, red = hBMP7 monomeric peptides). As shown by silver staining in reducing conditions (+DTT), in the case of BMP4, thrombin (T) gives rise to a single band, suggesting a single cleavage event. In contrast plasmin (P) cleavage results in two bands, suggesting multiple cleavages. In the case of BMP7, both thrombin and plasmin give rise to two bands each. However, thrombin and plasmin derived bands run at different molecular weights, indicating different specificity of the proteases.

(C) Activity assay of bacterially expressed BMP4/7. Bacterially expressed and purified recombinant hBMP4/7 was incubated with or without proteases (plasmin or thrombin). The specific activity of untreated and protease treated hBMP4/7 was measured in the newt myotube assay. Data are presented as mean ± SEM (n = 3).

(D) Multiple sequence alignment of human BMP2, BMP4, BMP5, BMP6 and BMP7. BMPs are sub-grouped according to their sequence homology.

Mature bovine BMP2 and BMP4 display sequence similarity. Mature bovine BMP5, BMP6 and BMP7 display sequence similarity. The alignments of mature bovine BMP protein sequences were obtained from using the ClustalW2 (http://www.ebi.ac.uk/Tools/services/web/toolform.ebi?tool=clustalw2) algorithm with standard parameters.

(E) Cartoon of mature human BMP4/4 homodimer. Arginine (R) and Lysine (K) residues are enlarged. BMP4 Monomers are connected by an intermolecular disulfide bond (brown dashed line) at Cysteine (C) C81. Three intramolecular disulfide bonds (green, dashed lines) are formed between C16-C80, C45-C113, C49-C115 in each of the monomers.

Figure S4

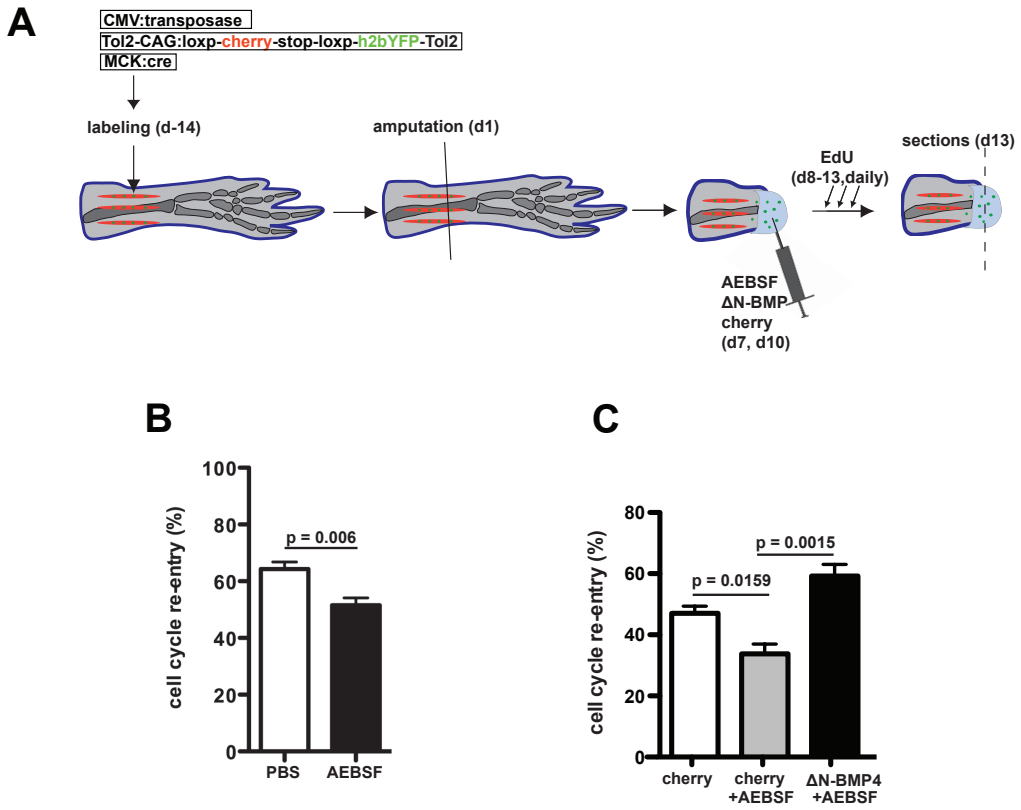

Figure S4. Serine proteases act upstream of BMPs to promote cell cycle entry of dedifferentiating myofibers. Relates to Figure 4.
(A) Representation of the experiment testing the effect of protease inhibition and BMP rescue on muscle dedifferentiation in vivo. The plasmin/thrombin inhibitor AEBSF or control PBS was injected together with baculovirus overexpressing ΔN-BMP4 or Cherry into the blastema at 6dpa and 9dpa. Cell-cycle re-entry was quantified by EdU incorporation in the YFP+ myofiber progeny at 13dpa.
(B) AEBSF reduces the cell-cycle re-entry of YFP+ cells in the blastema. Data are presented as mean ± SEM (n = 6-8 limbs). Significance calculated by Student's t-test.
(C) Viral-mediated overexpression of ΔN-BMP4 rescues the suppression of muscle cell cycle re-entry by AEBSF-mediated protease inhibition. Data are presented as mean ± SEM (n = 8 limbs). Significance calculated by Student's t-test.

Supplemental Tables

Table S1

N	Protein Name	Gene Identifier(s)	Peptides Detected by Mass Spectrometry		
			Sequence*	m/z	MASCOT peptide ions score
1	Bone Morphogenetic Protein 2	gi|7c149642861 gi|7c148744883 gi|7c157279020 gi|7c296481187 gi|7c153850483	K.NYQDMVVEGCGCR.-	802.5	64
2	Bone Morphogenetic Protein 4	gi|7c57545008 gi|7c68445390 gi|7c114052743 gi|7c109818952 gi|7c86821122 gi|7c296483082	K.NYQEMVVEGCGCR.- K.NYQEMVVEGCGCR.-	801.5 809.3	85 63
3	Bone Morphogenetic Protein 5	gi|7c194677539 gi|7c297488876 gi|7c296474598	K.LNAISVLYFDDSSNVILK.K R.MSSVGDYNTSEQK.Q R.MSSVGDYNTSEQK.Q K.KHELYVSFR.D** K.HELYVSFR.D**	1006.3 723.6 731.6 394.0 526.0	70 89 91 36 33
4	Bone Morphogenetic Protein 6	gi|7c194677896 gi|7c297489529 gi|7c296473962	R.ASSASDYNSSELK.T	680.1	64
5	Bone Morphogenetic Protein 7	gi|7c76633049 gi|7c297481860 gi|7c296480909	R.VANVAENSSSDQR.Q K.KHELYVSFR.D** K.HELYVSFR.D**	689.1 394.0 526.1	84 36 33

Table S1. Bone morphogenetic proteins identified in BMP4 immunoprecipitation by mass spectrometry. Relates to Figure 2.

(*) M refers to methionine oxidized and C refers to cystein carbamidomethylated.

(**) Stretches are identical in BMP5 and BMP7 sequences.

Supplemental Tables (separate .xlsx files)

Table S2. Edman sequencing of rhBMPs. Relates to Figure 2 Figure S3 and Data S1.
Numerical data derived from Edman sequencing trace seen in Data S1 of rhBMP4/4 untreated/+plasmin/+thrombin as well as rhBMP4/7 + plasmin are presented for individual Edman cycles (1-5).

Table S3. **Bovine BMP peptides identified by mass spectrometry. Relates to Figure 1 and Figure S1.**
Table of the 34 proteins identified by MS from the gel slice of the final purification step. Peptides were identified by mass spectrometry of a non-reducing gel slice spanning 28-39 kD. Bovine BMP peptides that were identified mapped onto protein sequences of the complete precursor protein.

Supplemental Data (separate .pdf file)

Data S1. Traces of Edman sequencing of rhBMPs. Relates to Figure 2, Figure S3 and TableS2.
Edman traces of rhBMP4/4 untreated/+plasmin/+thrombin as well as rhBMP4/7 + Plasmin are shown for individual Edman cycles (1-5). Colored circles (red, green, orange, blue, pink) highlight major amino acid peaks identified for each individual cycle. The corresponding colored circles in successive traces delineate a peptide that matches a BMP peptide sequence. Black circles highlight minor abundance amino acids that could not be assigned to the BMP query sequence and are most likely contamination.

Data S1

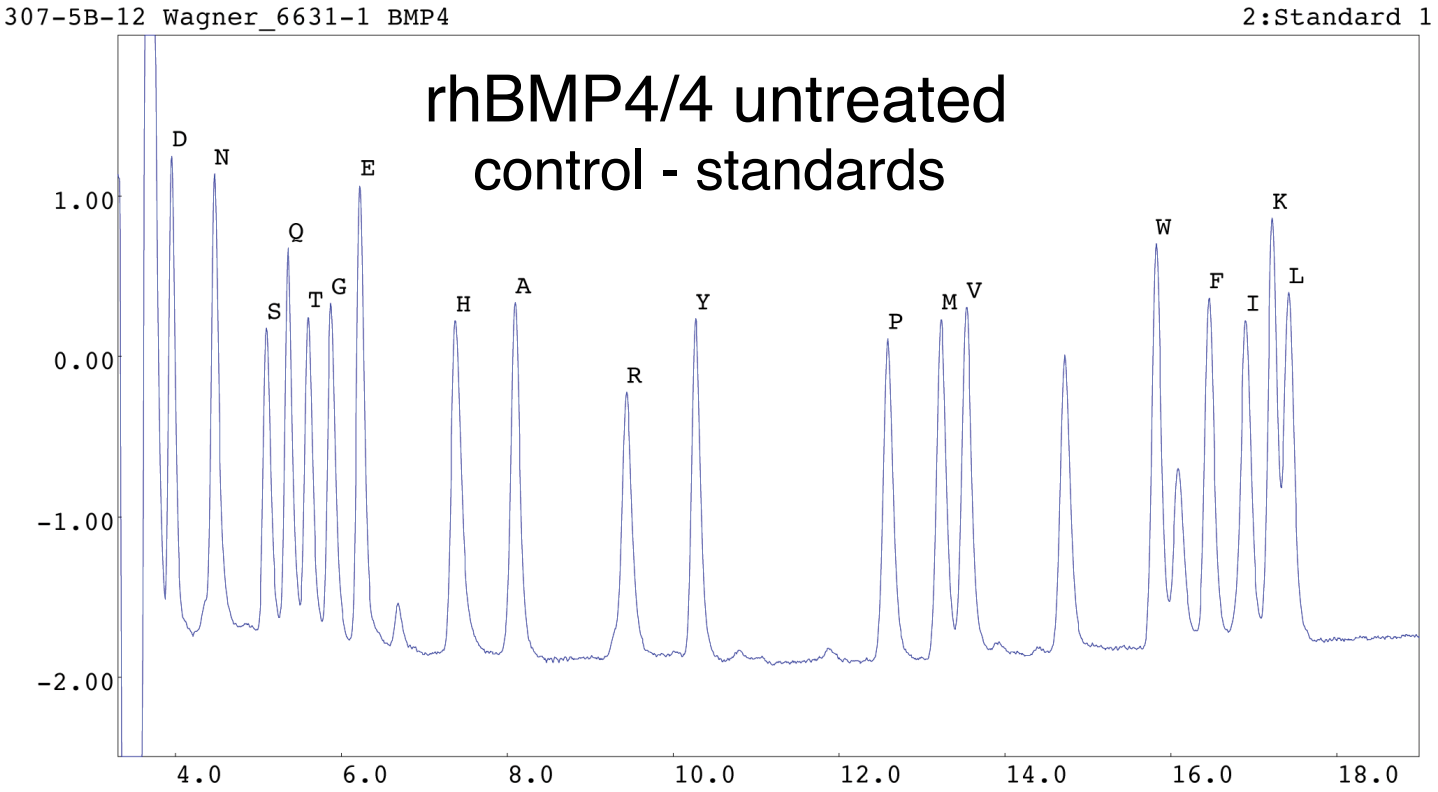
307-5B-12 Wagner_6631-1 BMP4
2:Standard 1
rhBMP4/4 untreated
control - standards
1.00
0.00
-1.00
-2.00
D
N
S
Q
T
G
E
H
A
R
Y
P
M
V
W
F
I
K
L
4.0
6.0
8.0
10.0
12.0
14.0
16.0
18.0

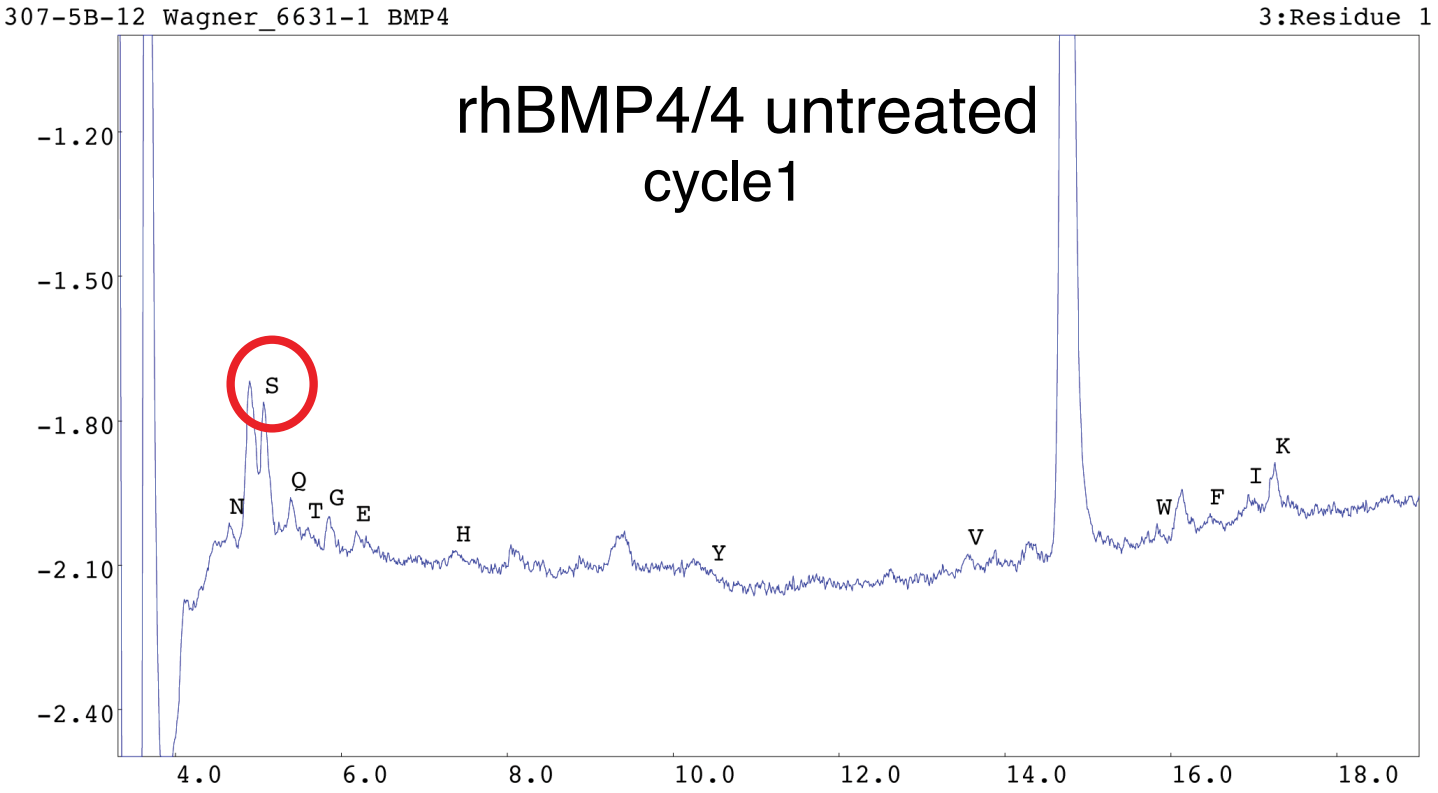
307-5B-12 Wagner_6631-1 BMP4
3:Residue 1
rhBMP4/4 untreated
cycle1
-1.20
-1.50
-1.80
-2.10
-2.40
S
N
Q
T
G
E
H
Y
V
W
F
I
K
4.0
6.0
8.0
10.0
12.0
14.0
16.0
18.0

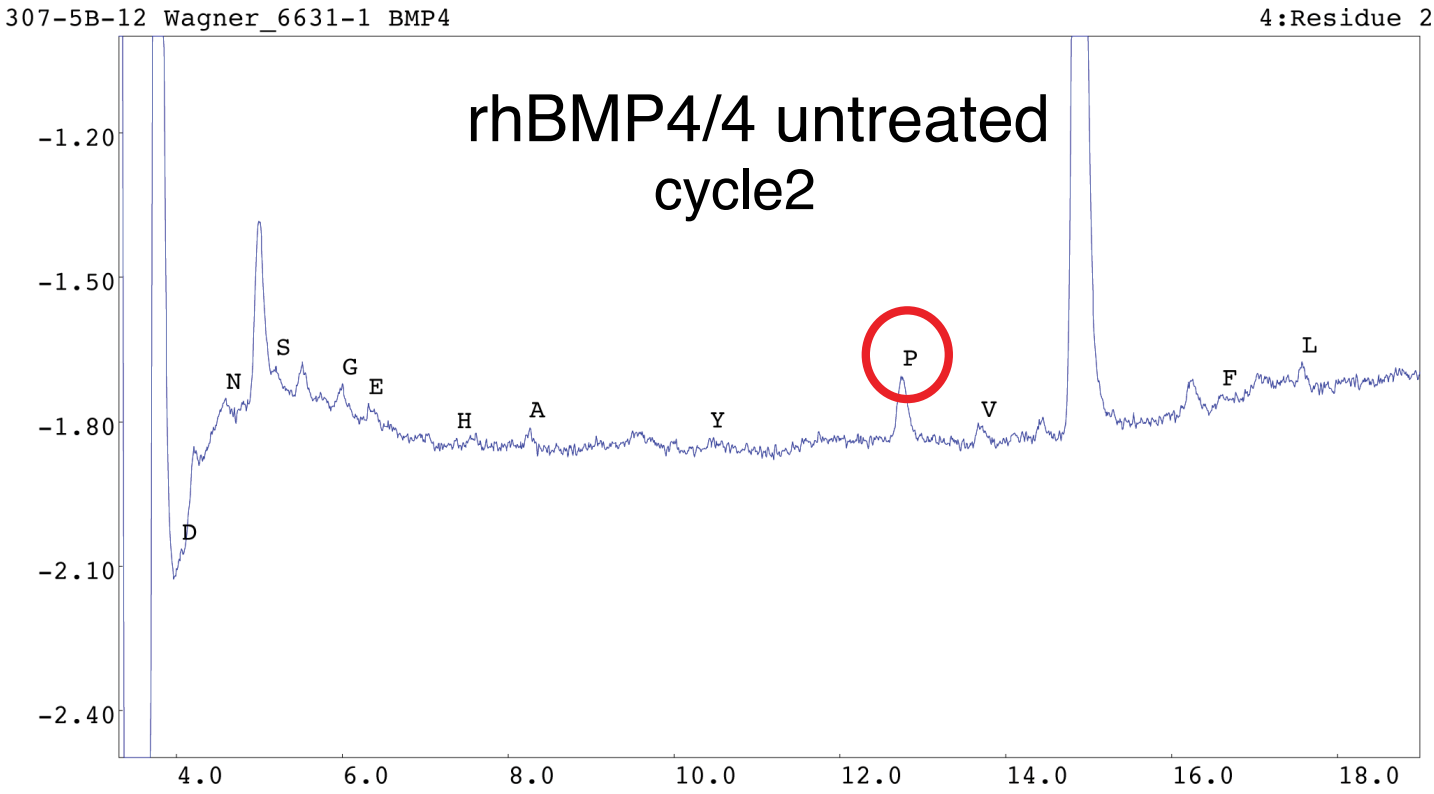
307-5B-12 Wagner_6631-1 BMP4
4:Residue 2
rhBMP4/4 untreated
cycle2
-1.20
-1.50
-1.80
-2.10
-2.40
4.0
6.0
8.0
10.0
12.0
14.0
16.0
18.0
D
N
S
G
E
H
A
Y
P
V
F
L

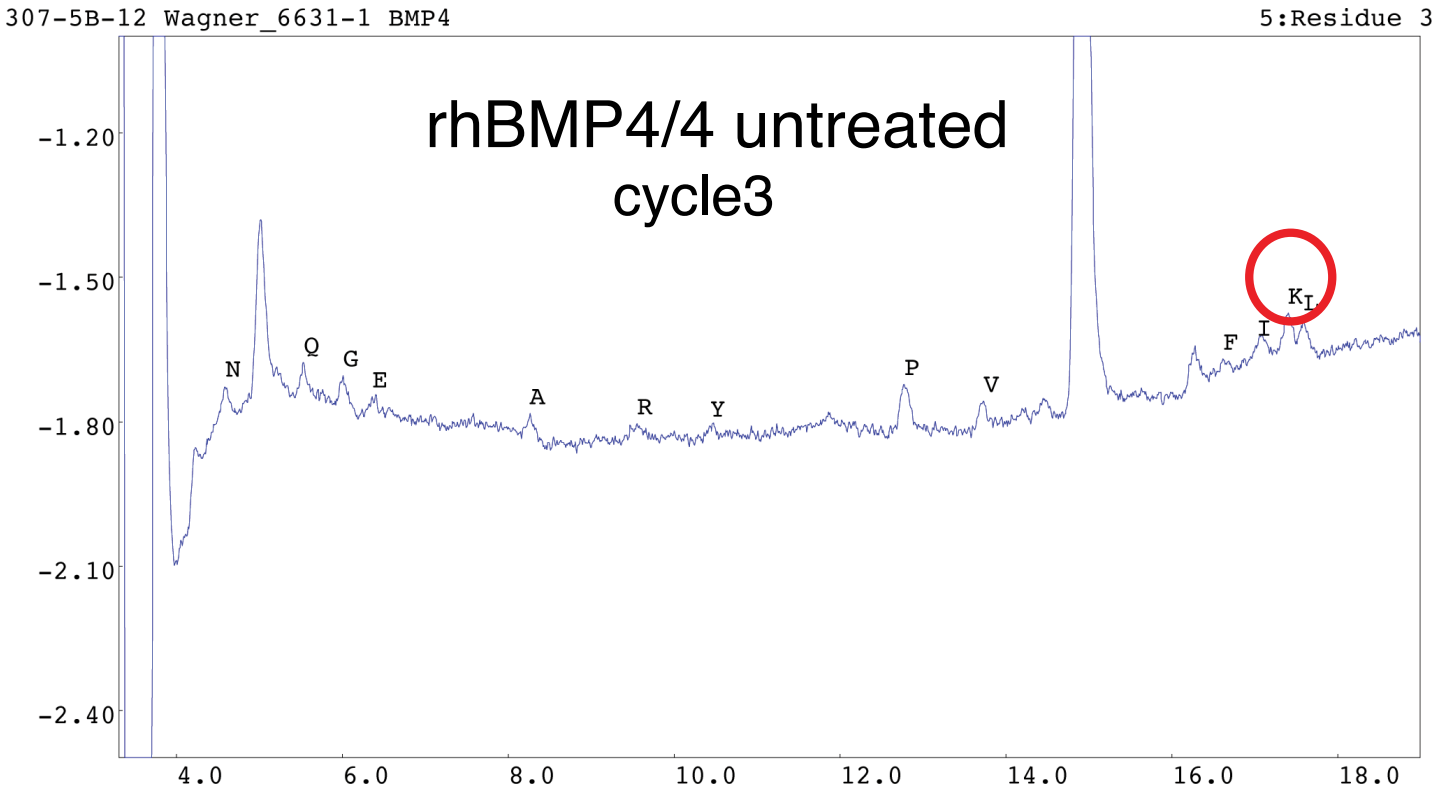
307-5B-12 Wagner_6631-1 BMP4
5:Residue 3
rhBMP4/4 untreated
cycle3
-1.20
-1.50
-1.80
-2.10
-2.40
4.0
6.0
8.0
10.0
12.0
14.0
16.0
18.0
N
Q
G
E
A
R
Y
P
V
F
I
K
L

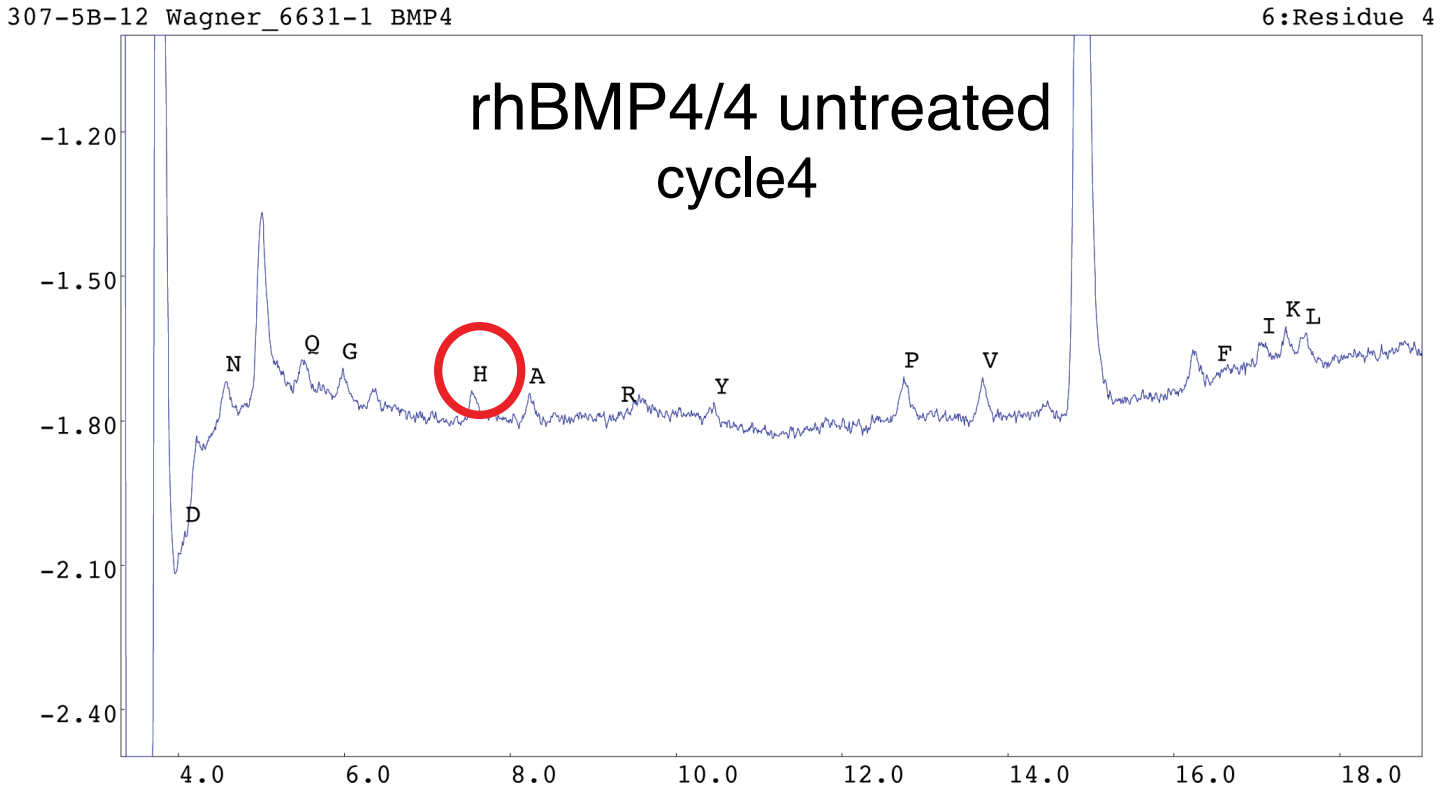
307-5B-12 Wagner_6631-1 BMP4
6:Residue 4
rhBMP4/4 untreated
cycle4
-1.20
-1.50
-1.80
-2.10
-2.40
4.0
6.0
8.0
10.0
12.0
14.0
16.0
18.0
D
N
Q
G
H
A
R
Y
P
V
F
I
K
L

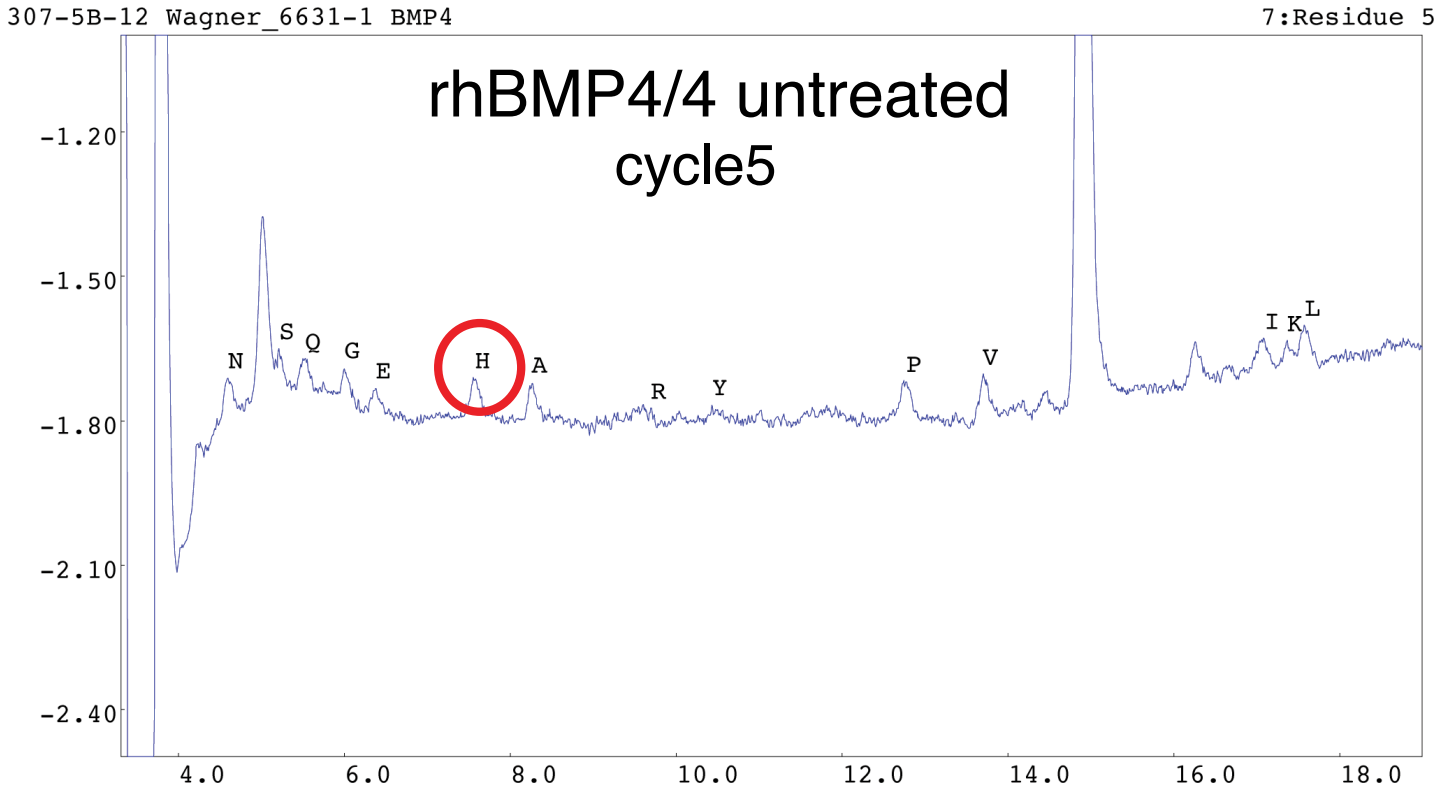
307-5B-12 Wagner_6631-1 BMP4
7:Residue 5
rhBMP4/4 untreated
cycle5
-1.20
-1.50
-1.80
-2.10
-2.40
4.0
6.0
8.0
10.0
12.0
14.0
16.0
18.0
N
S
Q
G
E
H
A
R
Y
P
V
I
K
L

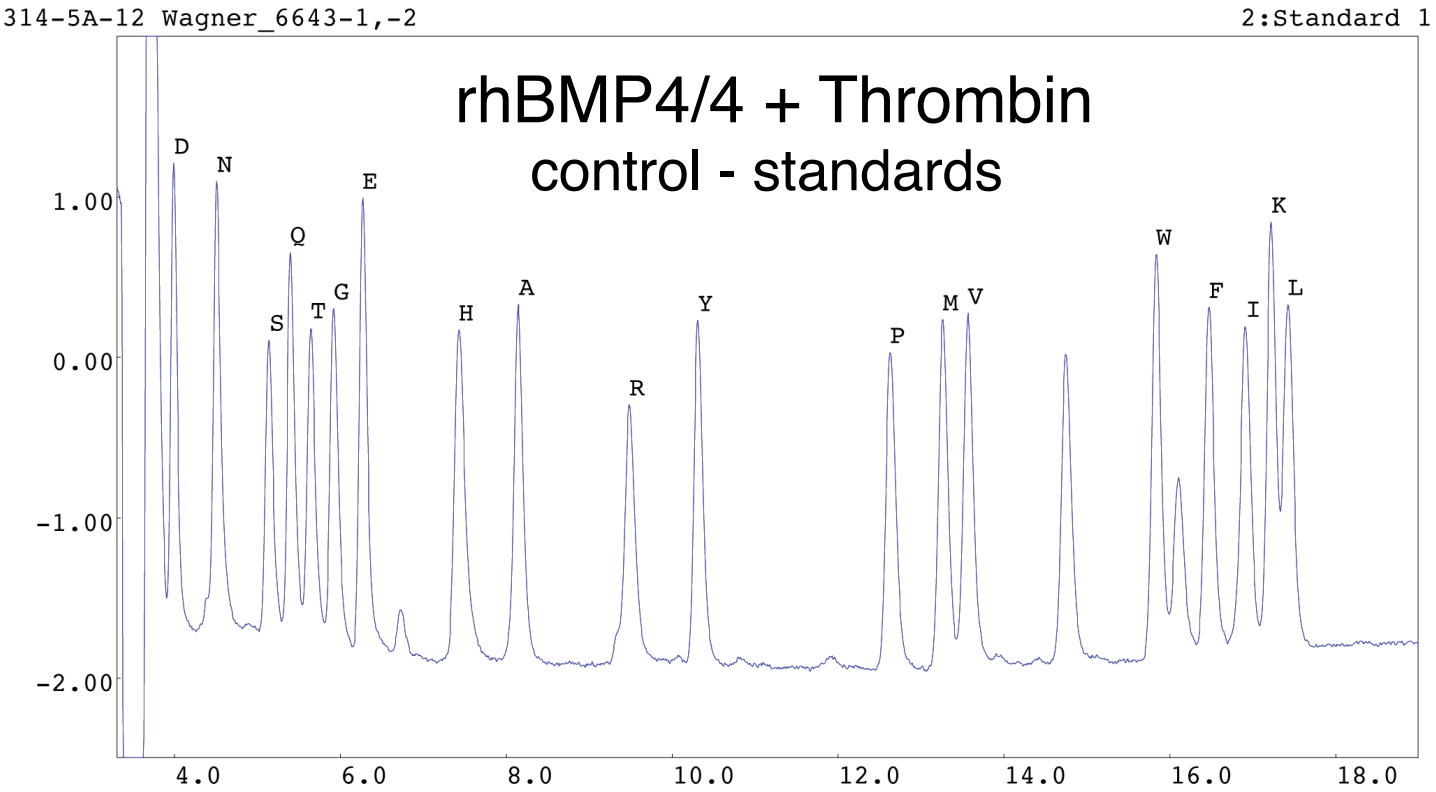
314-5A-12 Wagner_6643-1,-2
2:Standard 1
rhBMP4/4 + Thrombin
control - standards
D
N
E
Q
S
T
G
H
A
R
Y
P
M
V
W
F
I
K
L
1.00
0.00
-1.00
-2.00
4.0
6.0
8.0
10.0
12.0
14.0
16.0
18.0

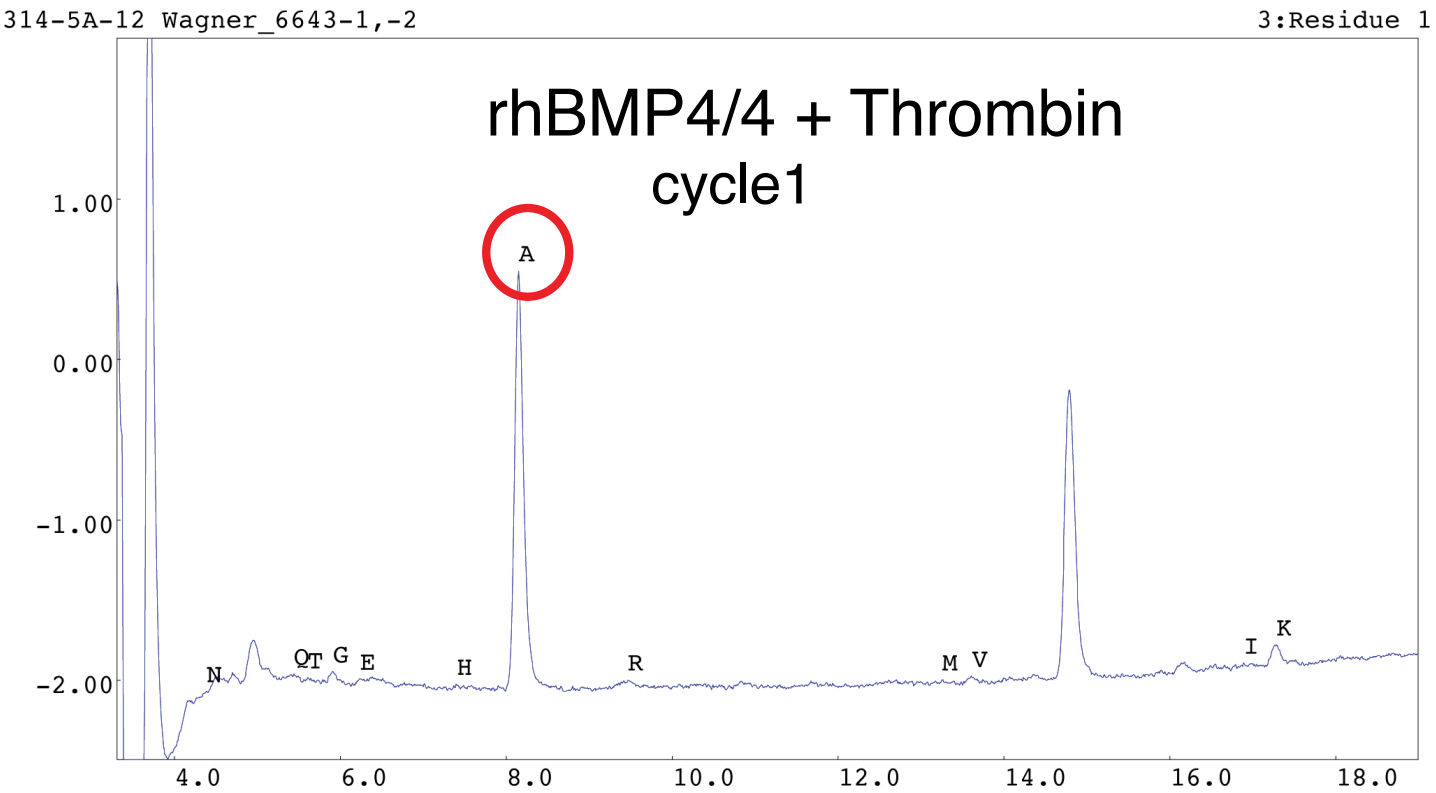
314-5A-12 Wagner_6643-1,-2
3:Residue 1
rhBMP4/4 + Thrombin
cycle1
A
N
Q
T
G
E
H
R
M
V
I
K
1.00
0.00
-1.00
-2.00
4.0
6.0
8.0
10.0
12.0
14.0
16.0
18.0

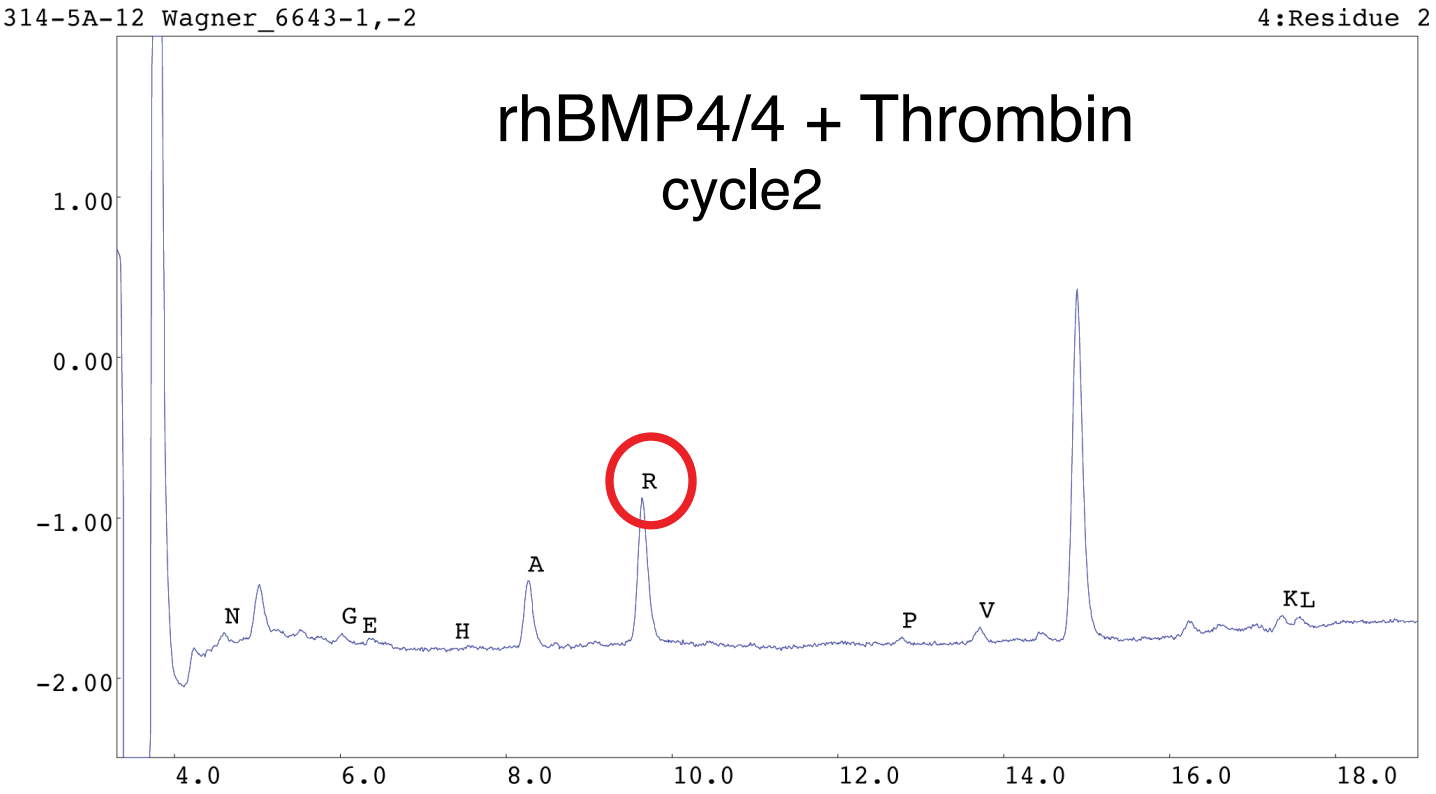
314-5A-12 Wagner_6643-1,-2
4:Residue 2
rhBMP4/4 + Thrombin
cycle2
1.00
0.00
-1.00
-2.00
N
G
E
H
A
R
P
V
KL
4.0
6.0
8.0
10.0
12.0
14.0
16.0
18.0

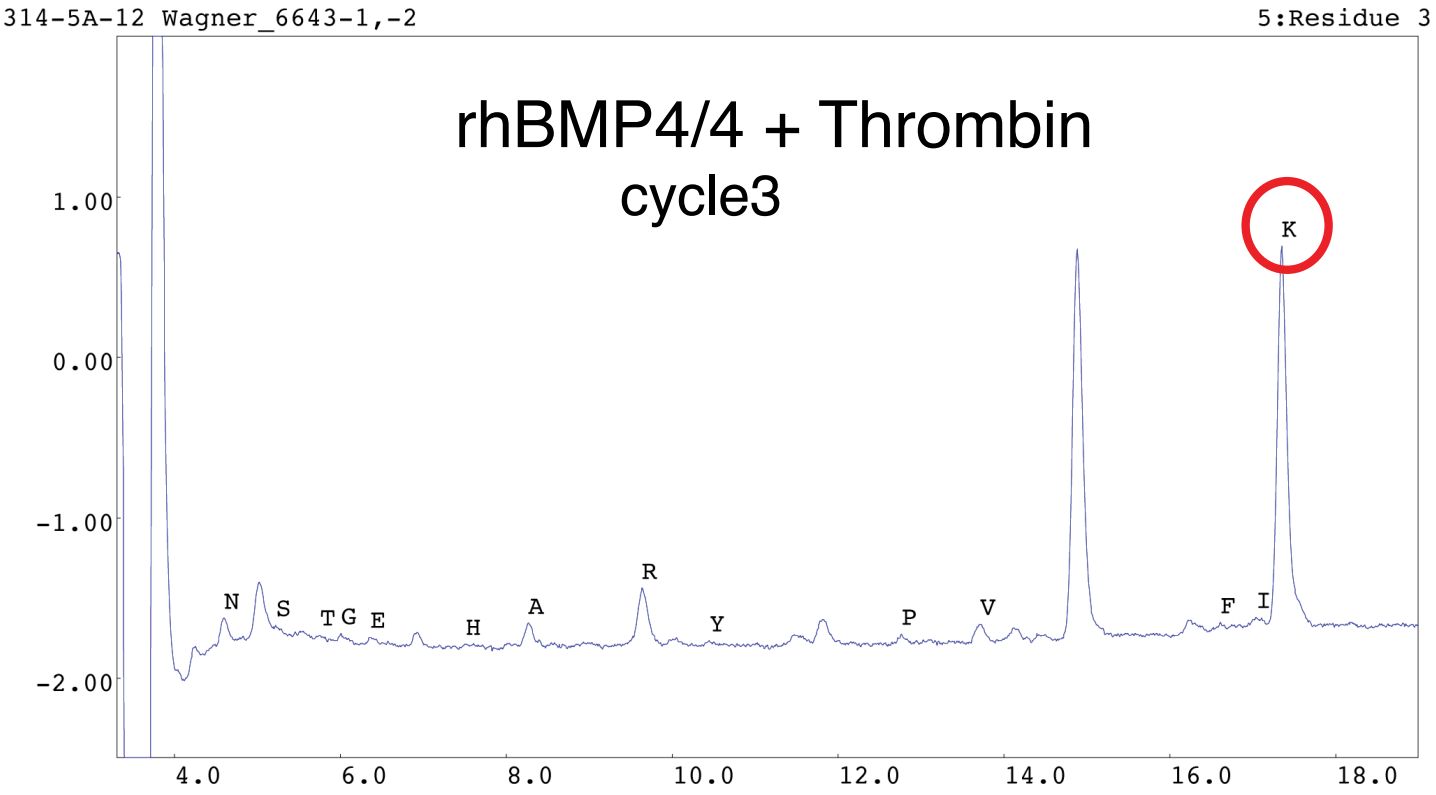
314-5A-12 Wagner_6643-1,-2
5:Residue 3
rhBMP4/4 + Thrombin
cycle3
1.00
0.00
-1.00
-2.00
N
S
TG
E
H
A
R
Y
P
V
F
I
K
4.0
6.0
8.0
10.0
12.0
14.0
16.0
18.0

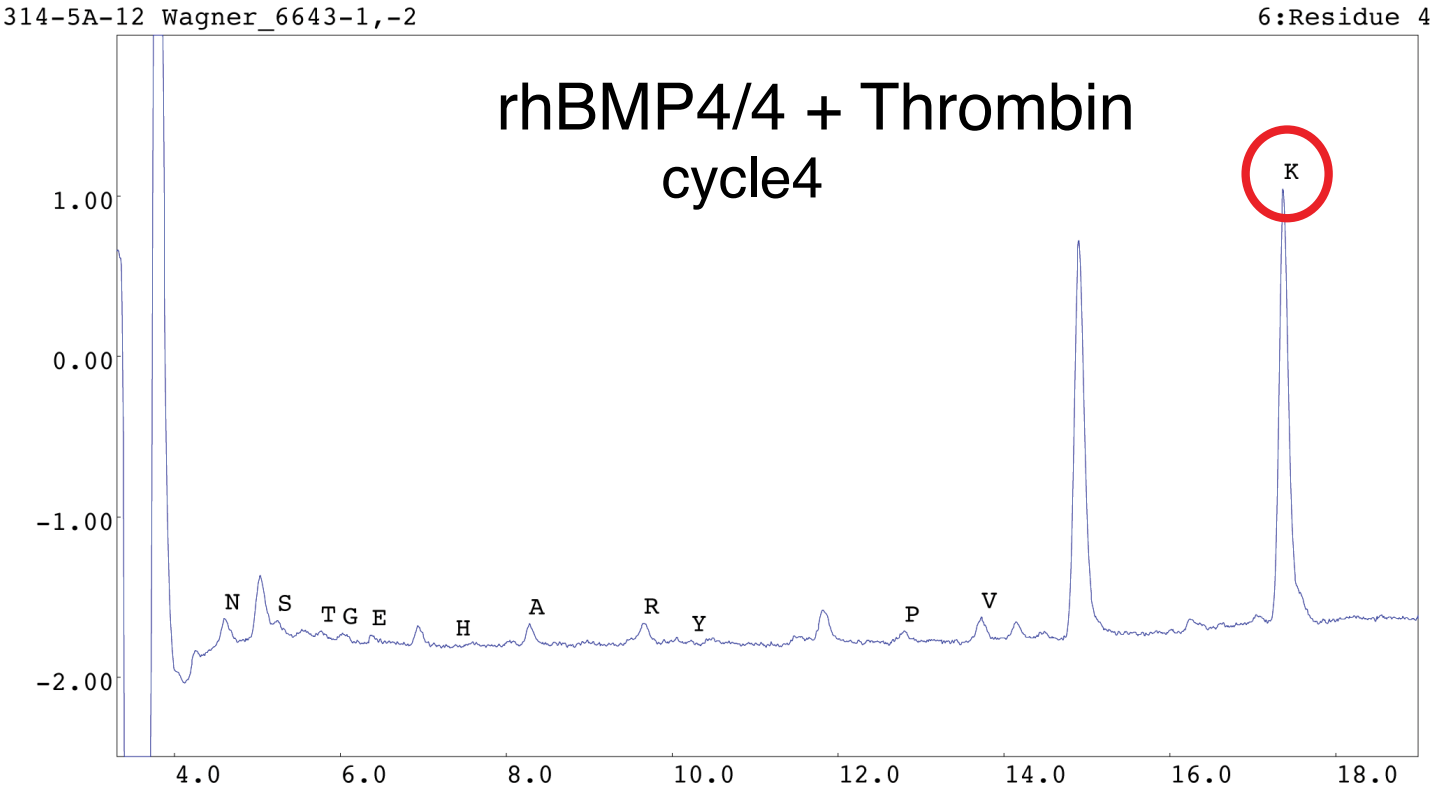
314-5A-12 Wagner_6643-1,-2
6:Residue 4
rhBMP4/4 + Thrombin
cycle4
K
1.00
0.00
-1.00
-2.00
N
S
T G E
H
A
R
Y
P
V
4.0
6.0
8.0
10.0
12.0
14.0
16.0
18.0

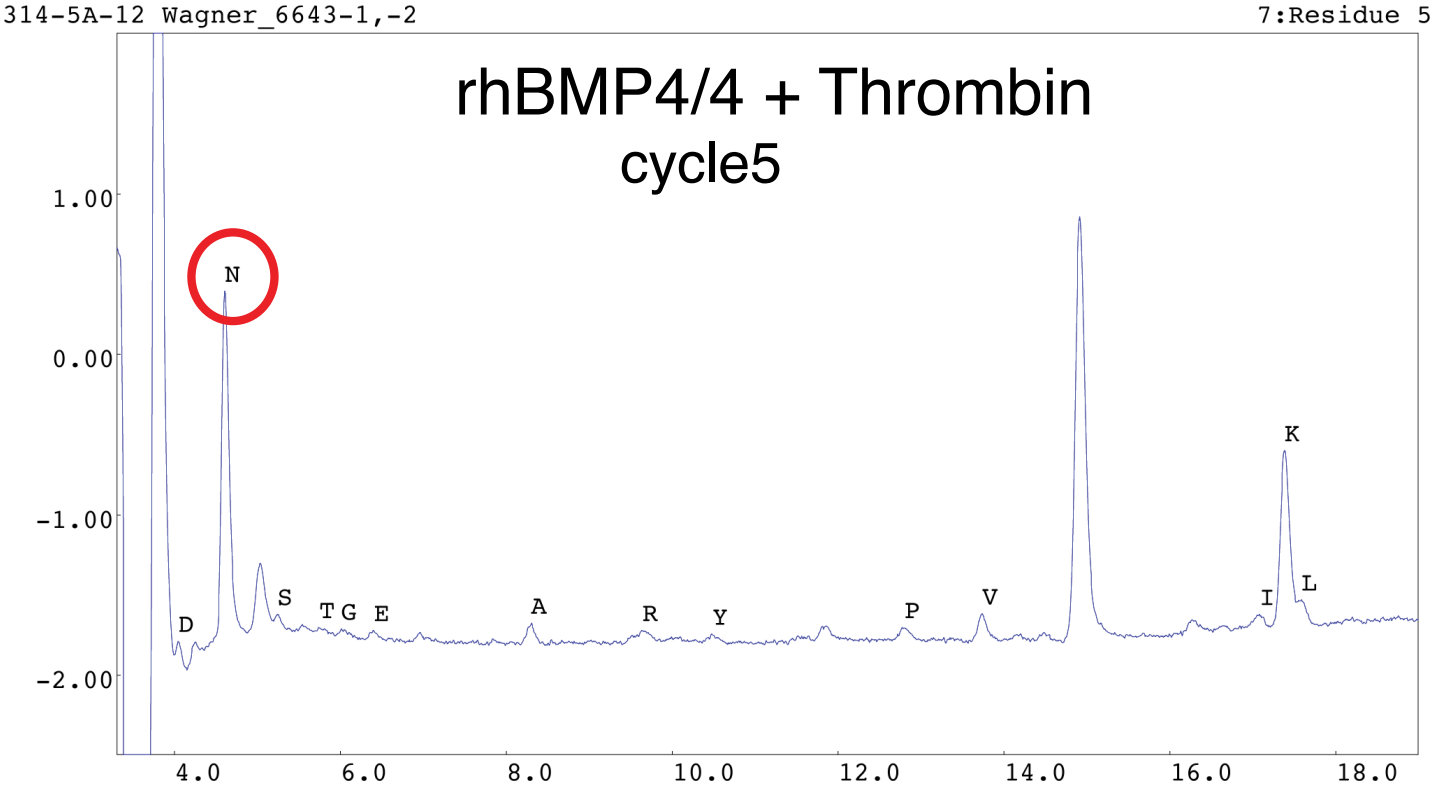
314-5A-12 Wagner_6643-1,-2
7:Residue 5
rhBMP4/4 + Thrombin
cycle5
N
1.00
0.00
-1.00
-2.00
K
D
S
T G E
A
R
Y
P
V
I
L
4.0
6.0
8.0
10.0
12.0
14.0
16.0
18.0

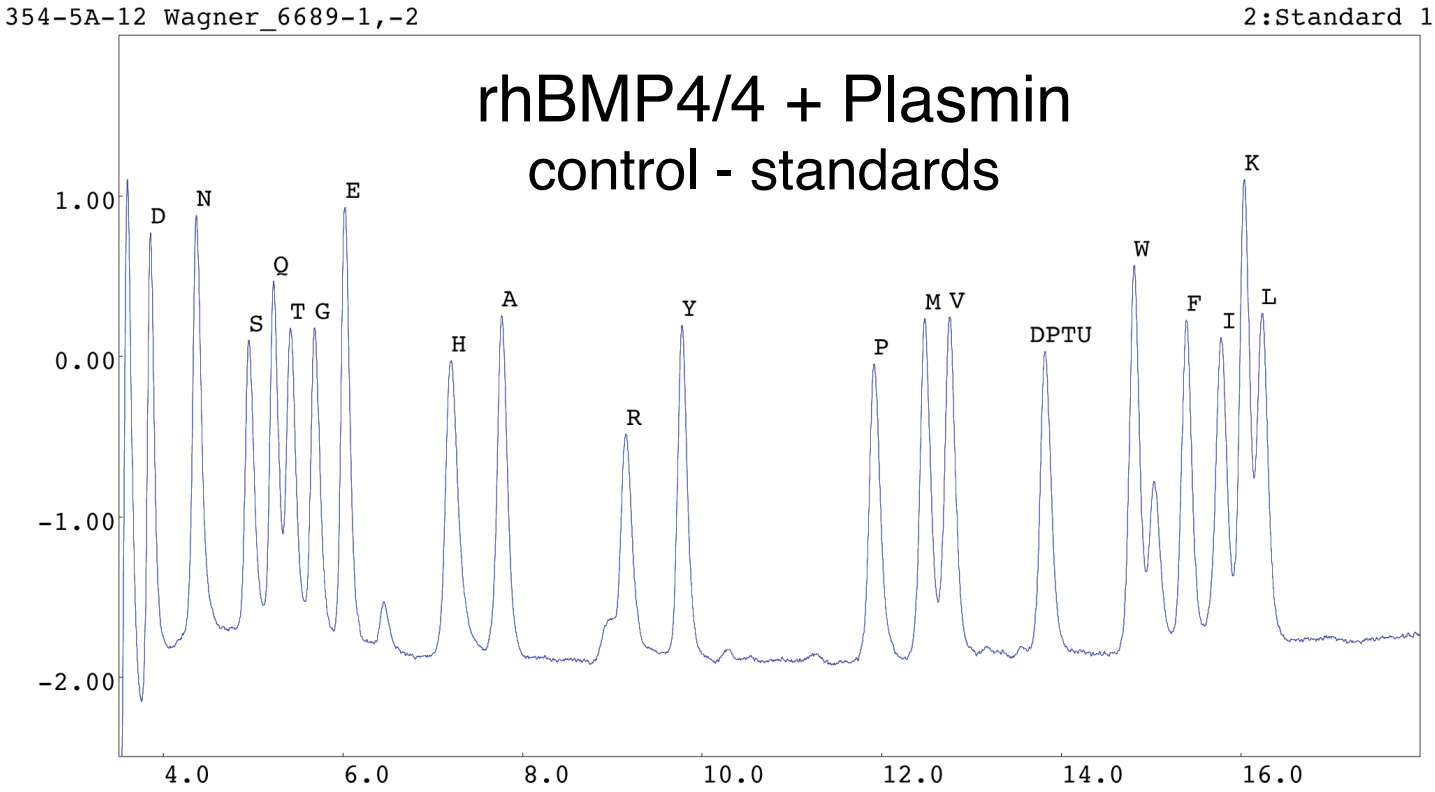
354-5A-12 Wagner_6689-1,-2
2:Standard 1
rhBMP4/4 + Plasmin
control - standards
1.00
0.00
-1.00
-2.00
D
N
E
Q
S
T G
H
A
R
Y
P
M V
DPTU
W
F
I
K
L
4.0
6.0
8.0
10.0
12.0
14.0
16.0

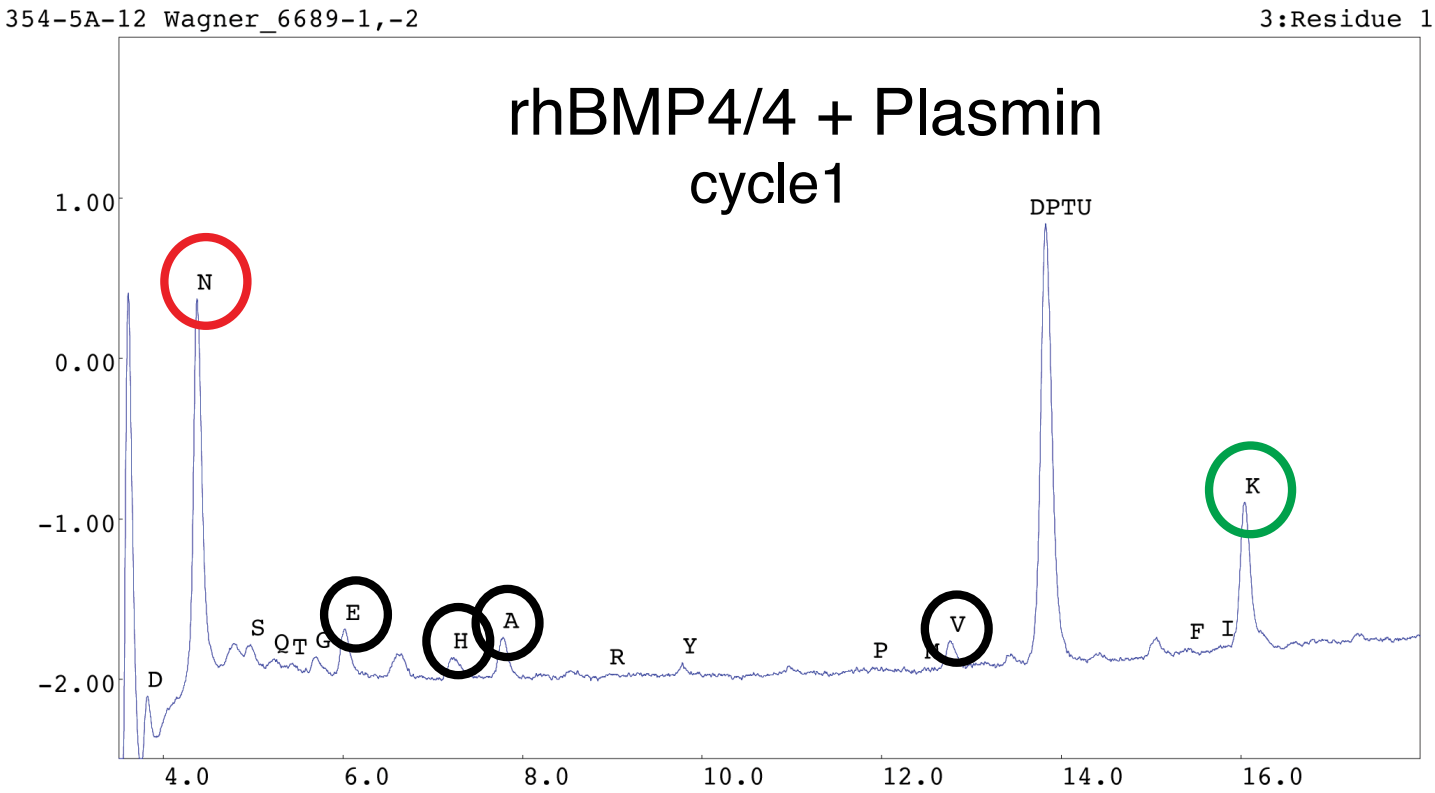
354-5A-12 Wagner_6689-1,-2
3:Residue 1
rhBMP4/4 + Plasmin
cycle1
1.00
0.00
-1.00
-2.00
N
DPTU
K
D
S
Q T G
E
H
A
R
Y
P
V
F I
4.0
6.0
8.0
10.0
12.0
14.0
16.0

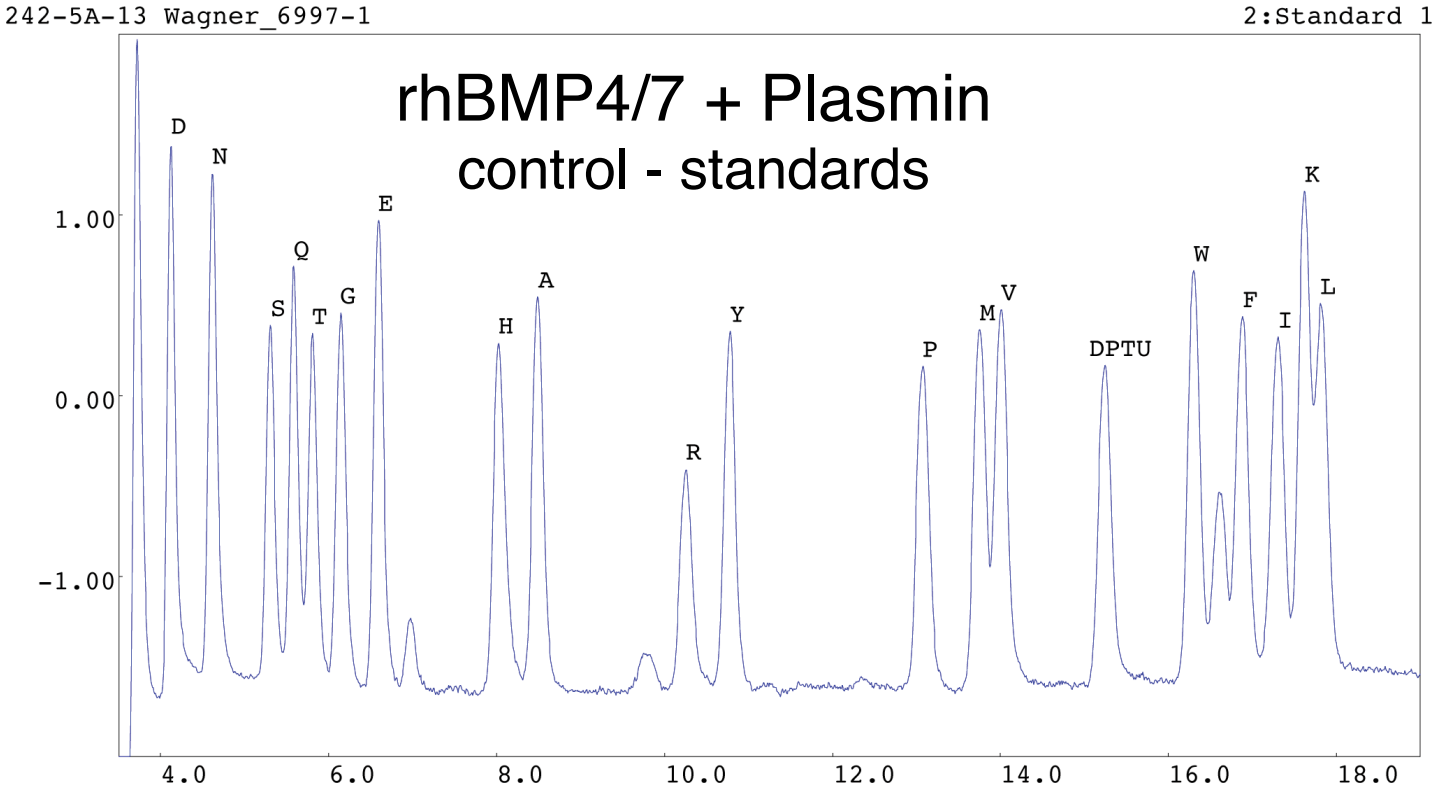
242-5A-13 Wagner_6997-1
2:Standard 1
rhBMP4/7 + Plasmin
control - standards
D
N
S
Q
T
G
E
H
A
R
Y
P
M
V
DPTU
W
F
I
K
L
1.00
0.00
-1.00
4.0
6.0
8.0
10.0
12.0
14.0
16.0
18.0

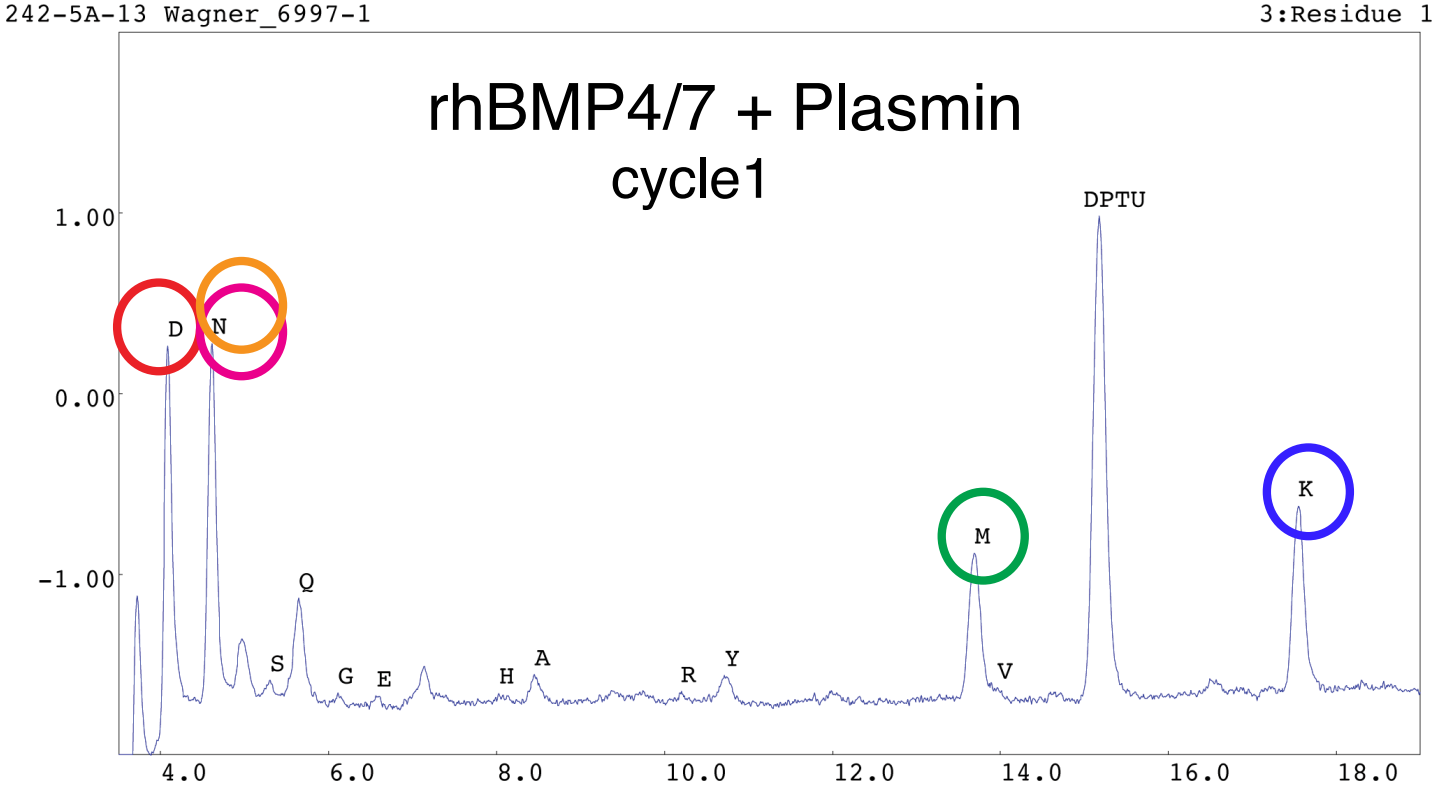
242-5A-13 Wagner_6997-1
3:Residue 1
rhBMP4/7 + Plasmin
cycle1
D
N
S
Q
G
E
H
A
R
Y
M
V
DPTU
K
1.00
0.00
-1.00
4.0
6.0
8.0
10.0
12.0
14.0
16.0
18.0

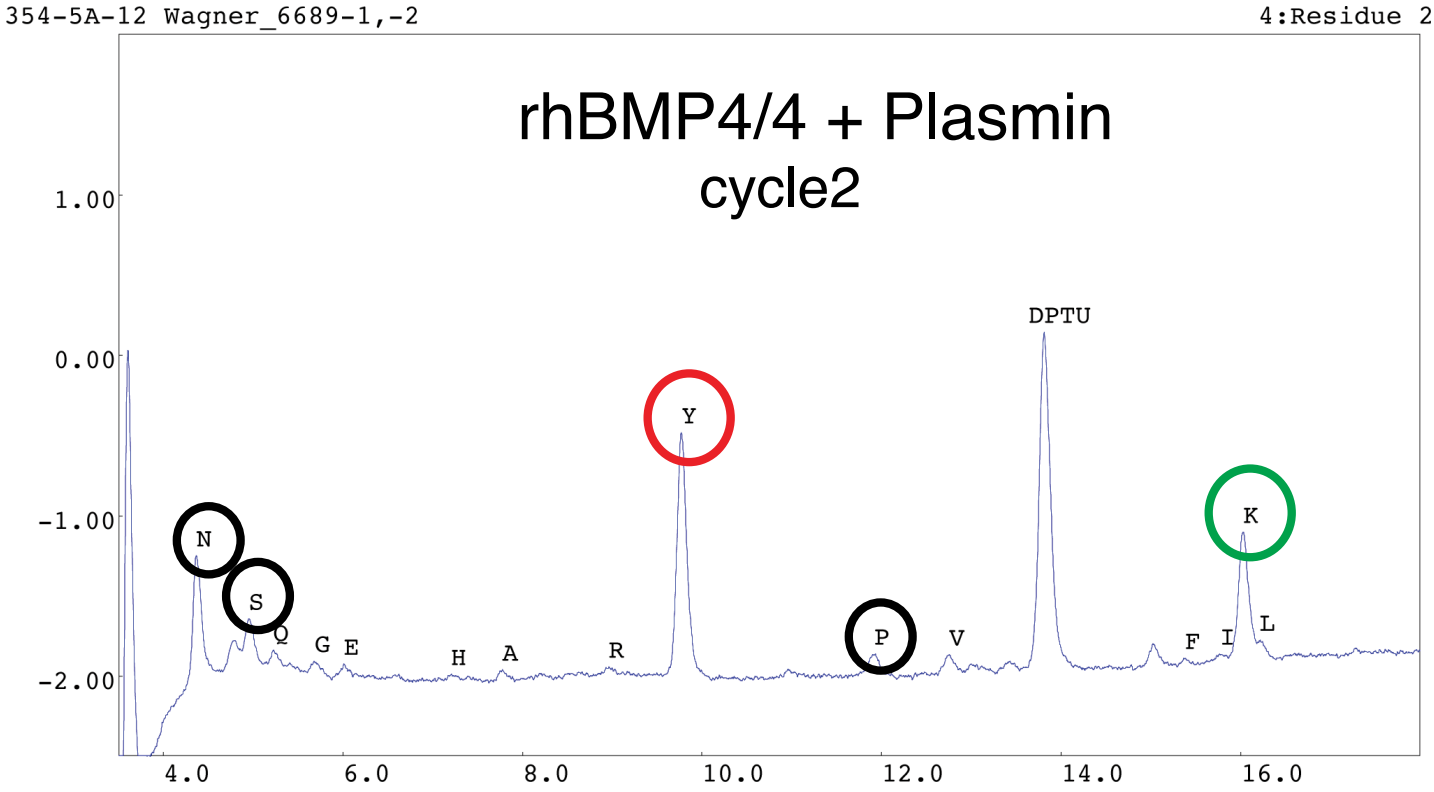
354-5A-12 Wagner_6689-1,-2
4:Residue 2
rhBMP4/4 + Plasmin
cycle2
1.00
0.00
-1.00
-2.00
DPTU
N
S
Q
G
E
H
A
R
Y
P
V
F
I
K
L
4.0
6.0
8.0
10.0
12.0
14.0
16.0

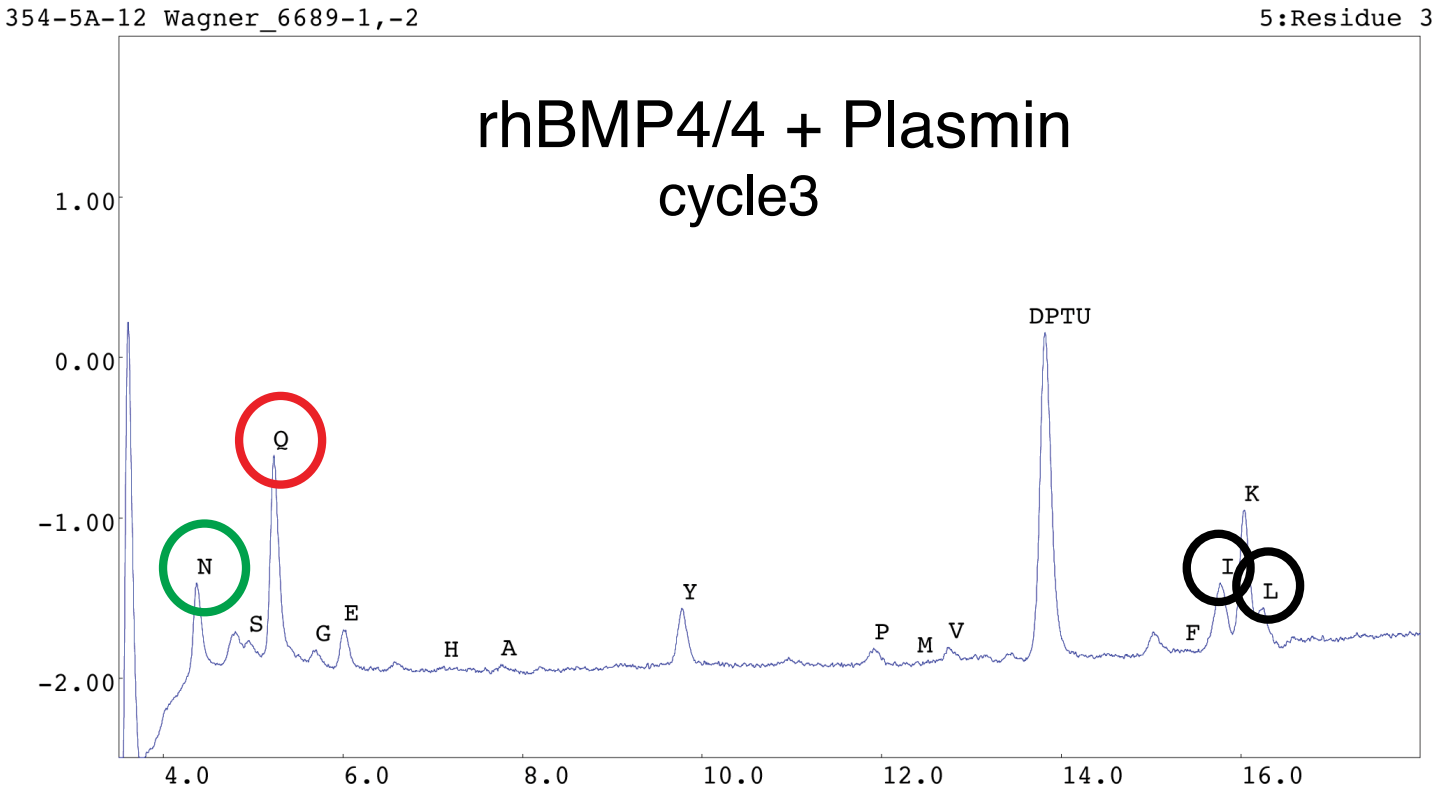
354-5A-12 Wagner_6689-1,-2
5:Residue 3
rhBMP4/4 + Plasmin
cycle3
1.00
0.00
-1.00
-2.00
DPTU
N
Q
S
G
E
H
A
Y
P
M
V
F
I
K
L
4.0
6.0
8.0
10.0
12.0
14.0
16.0

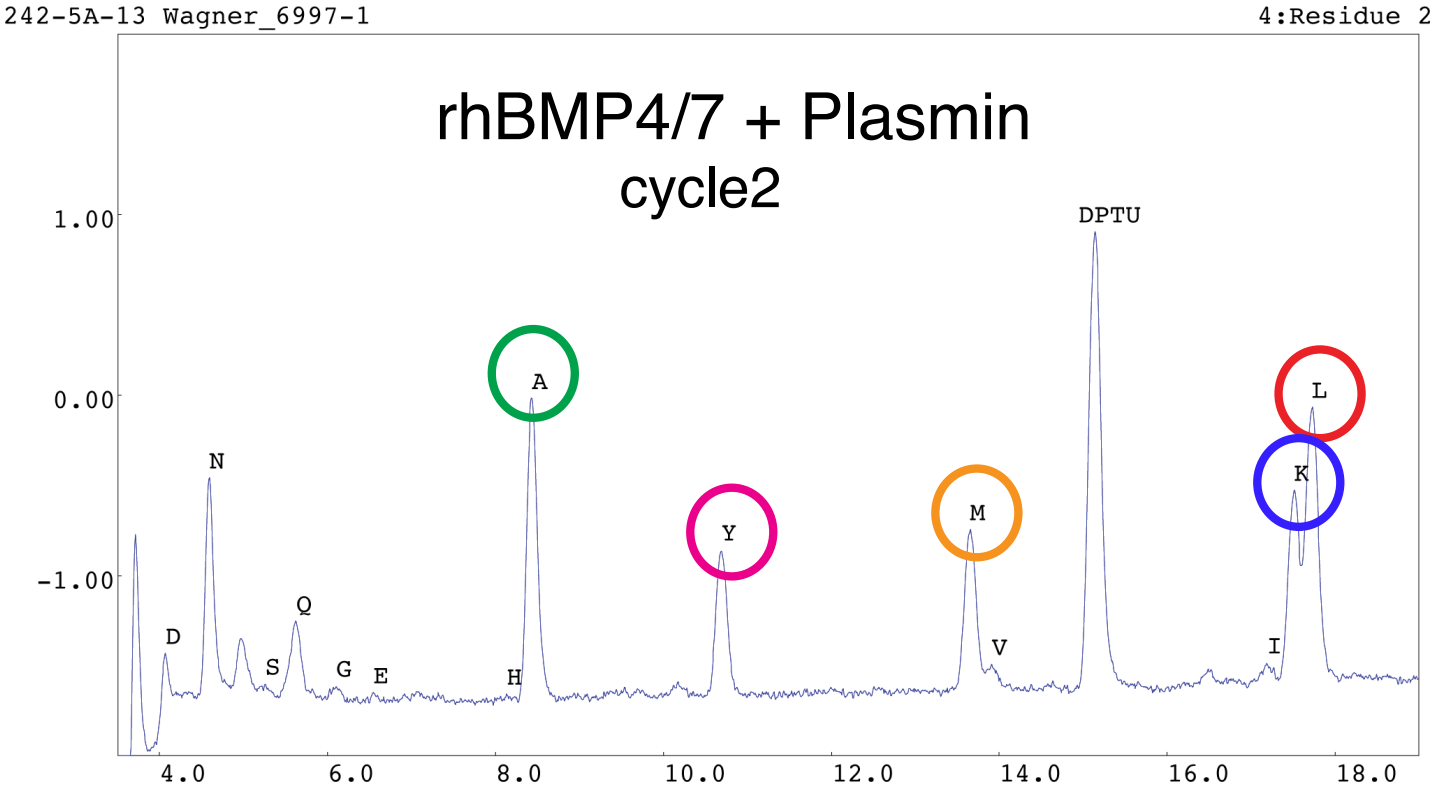
242-5A-13 Wagner_6997-1
4:Residue 2
rhBMP4/7 + Plasmin
cycle2
1.00
0.00
-1.00
4.0
6.0
8.0
10.0
12.0
14.0
16.0
18.0
D
N
S
Q
G
E
H
A
Y
M
V
DPTU
I
K
L

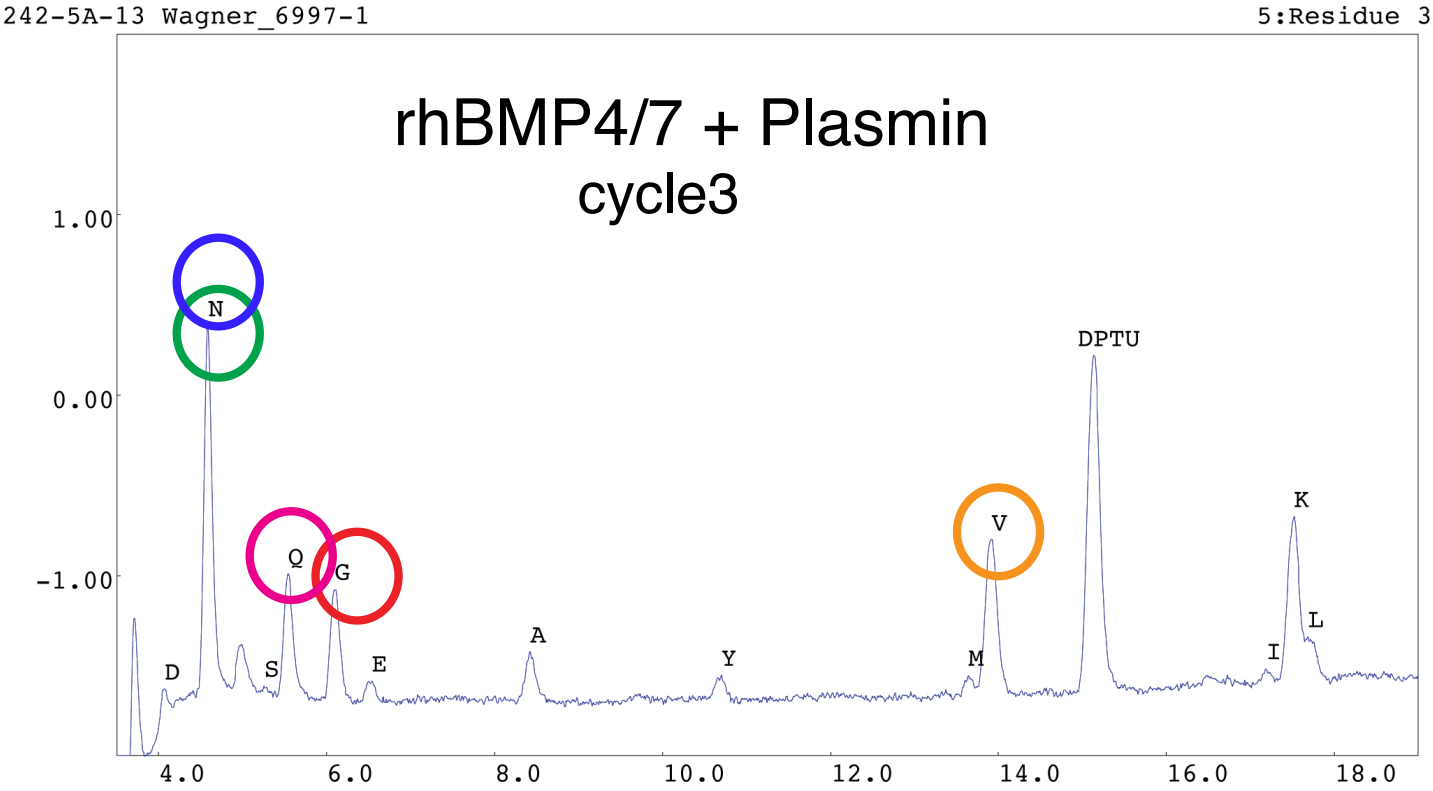
242-5A-13 Wagner_6997-1
5:Residue 3
rhBMP4/7 + Plasmin
cycle3
1.00
0.00
-1.00
4.0
6.0
8.0
10.0
12.0
14.0
16.0
18.0
D
N
S
Q
G
E
A
Y
M
V
DPTU
I
K
L

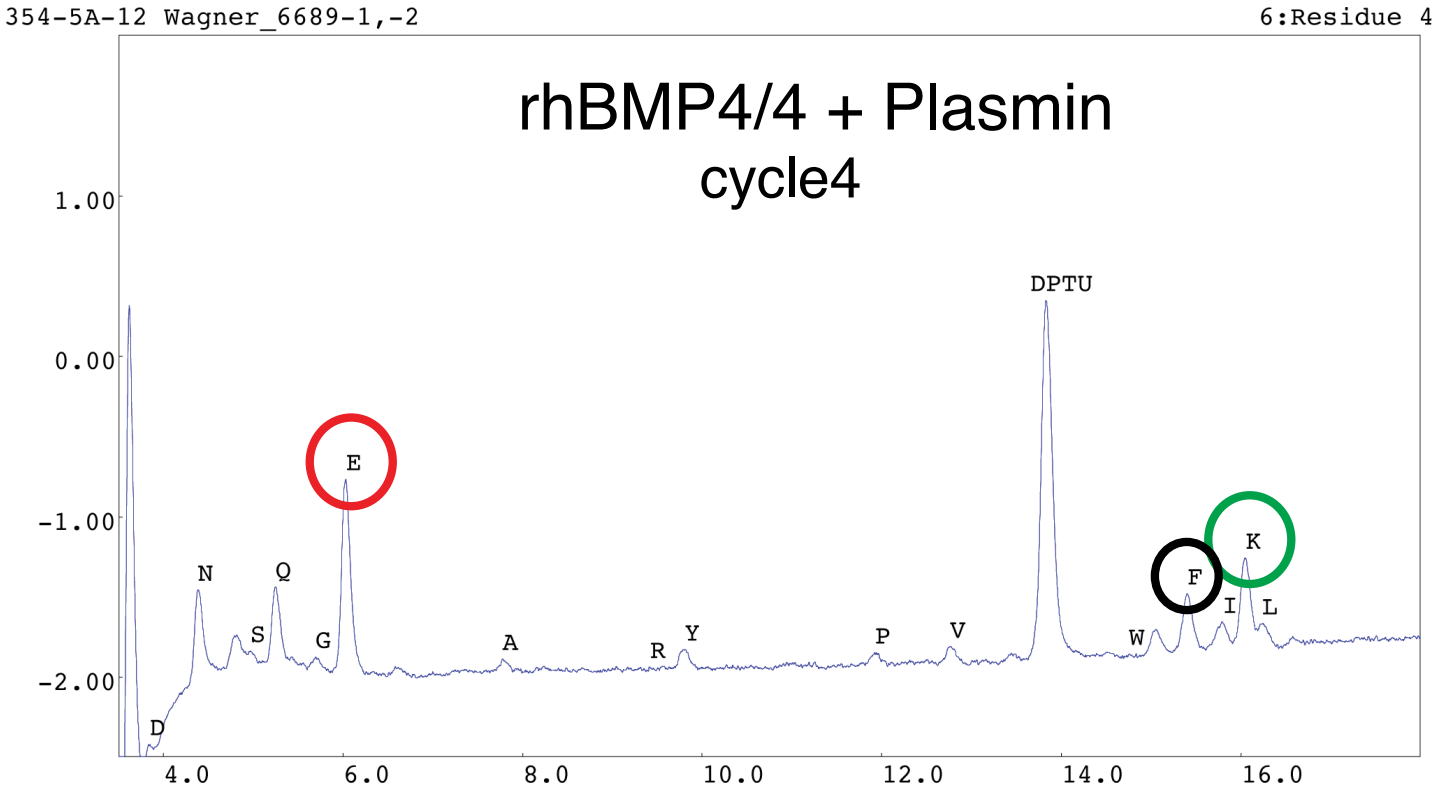
354-5A-12 Wagner_6689-1,-2
6:Residue 4
rhBMP4/4 + Plasmin
cycle4
1.00
0.00
-1.00
-2.00
4.0
6.0
8.0
10.0
12.0
14.0
16.0
DPTU
D
N
S
Q
G
E
A
R
Y
P
V
W
F
I
K
L

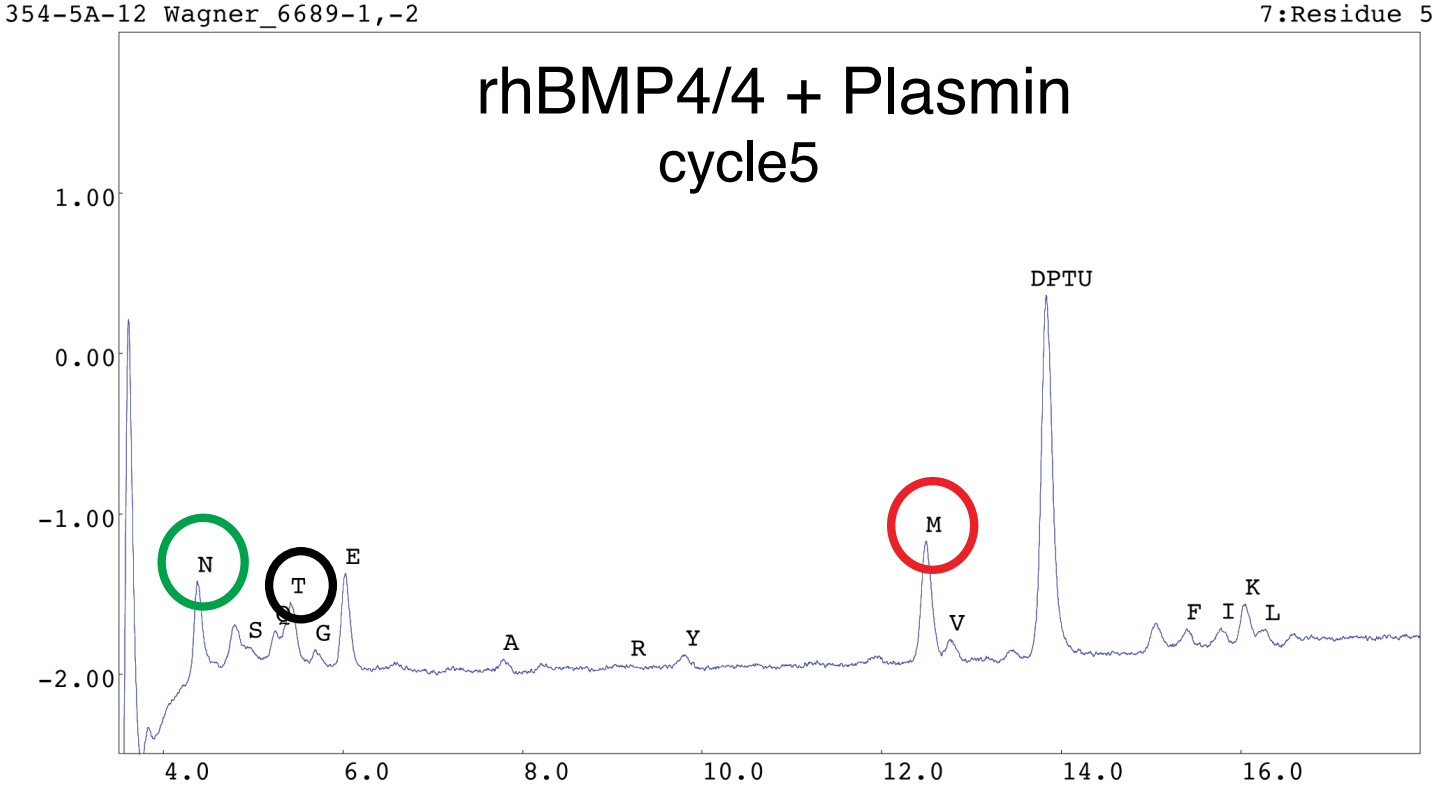
354-5A-12 Wagner_6689-1,-2
7:Residue 5
rhBMP4/4 + Plasmin
cycle5
1.00
0.00
-1.00
-2.00
4.0
6.0
8.0
10.0
12.0
14.0
16.0
DPTU
N
S
T
G
E
A
R
Y
M
V
F
I
K
L

242-5A-13 Wagner_6997-1 6:Residue 4

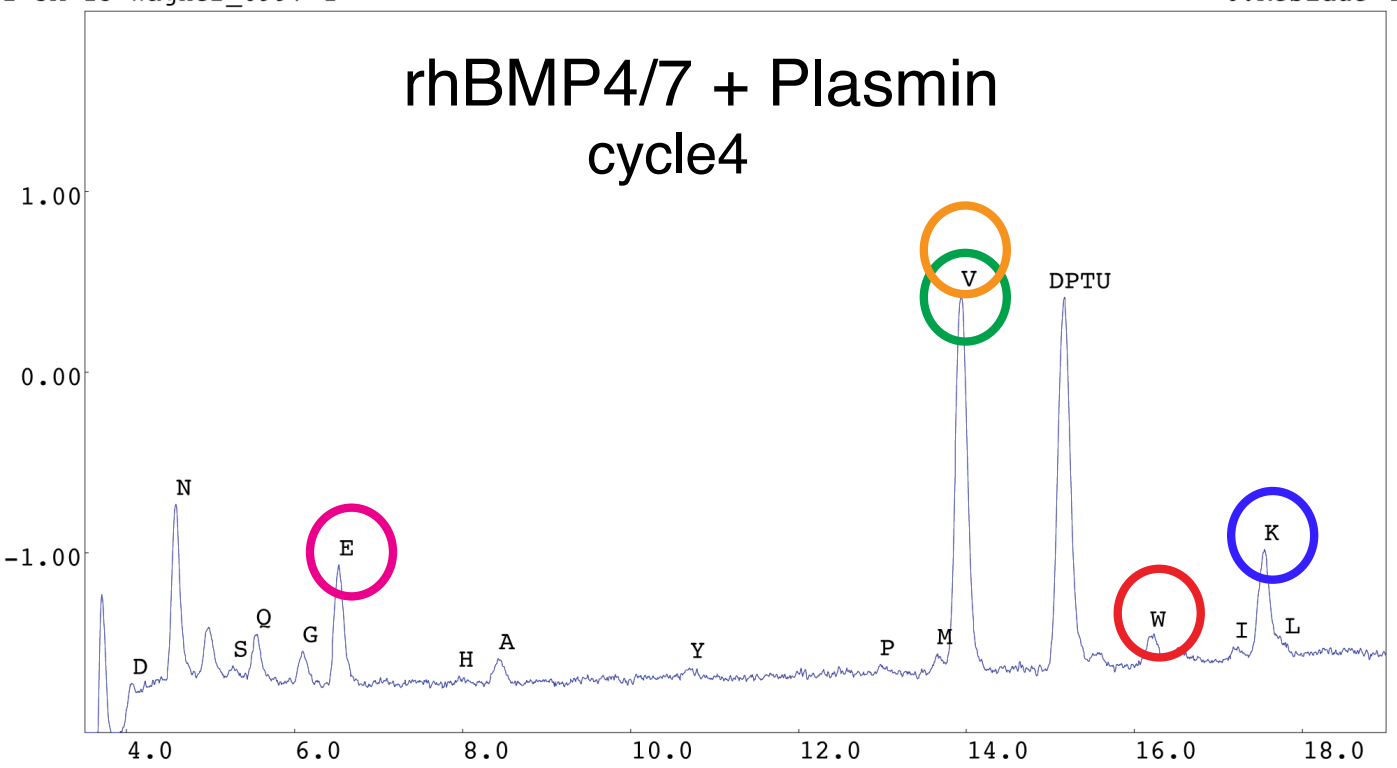

242-5A-13 Wagner_6997-1 7:Residue 5

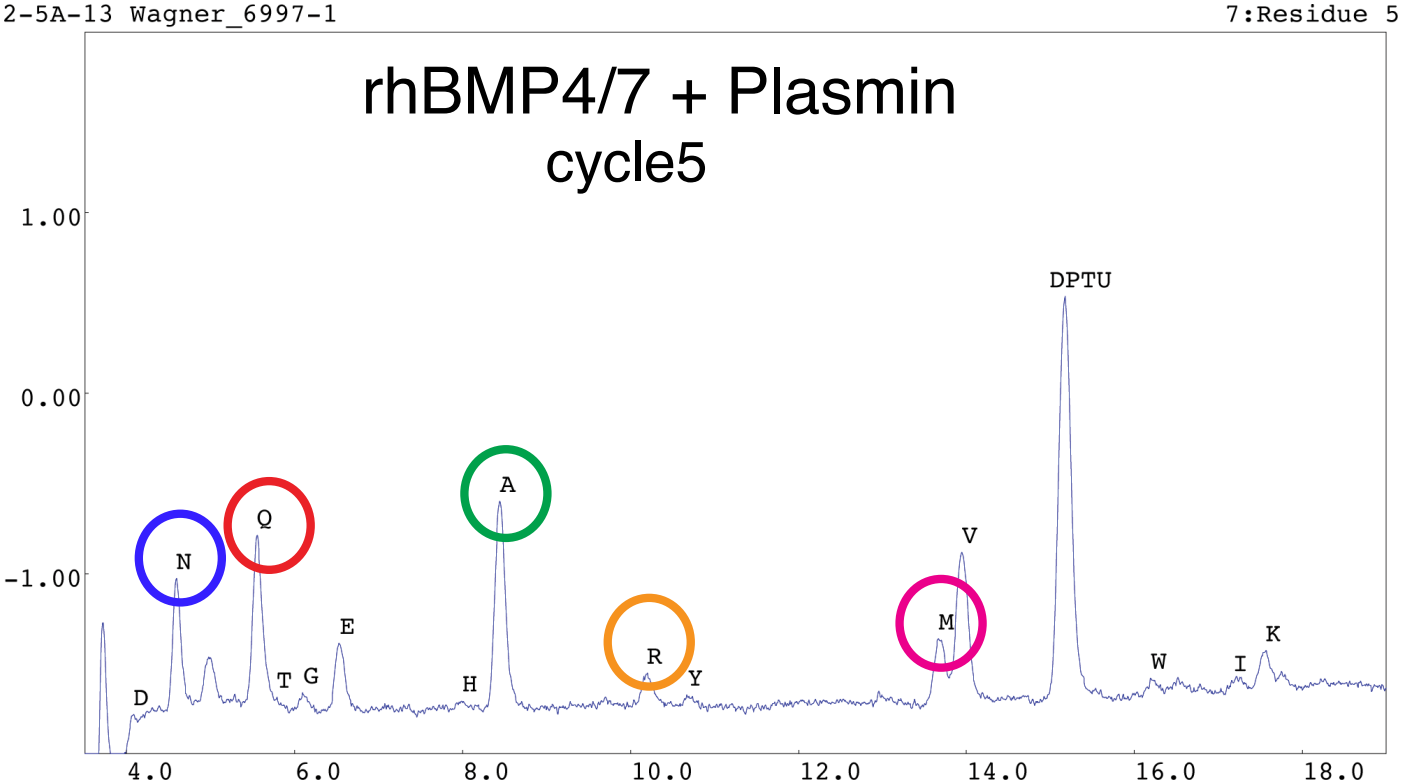

Data S1. Traces of Edman sequencing of rhBMPs. Relates to Figure 2, Figure S3 and TableS2.

Edman traces of rhBMP4/4 untreated/+plasmin/+thrombin as well as rhBMP4/7 + Plasmin are shown for individual Edman cycles (1-5). Colored circles (red, green, orange, blue, pink) highlight major amino acid peaks identified for each individual cycle. The corresponding colored circles in successive traces delineate a peptide that matches a BMP peptide sequence. Black circles highlight minor abundance amino acids that could not be assigned to the BMP query sequence and are most likely contamination.